



# Coupling of Fast Multipole Method and Microlocal Discretization for the 3-D Helmholtz Equation

Eric Darrigrand

## ► To cite this version:

Eric Darrigrand. Coupling of Fast Multipole Method and Microlocal Discretization for the 3-D Helmholtz Equation. 2001. hal-00133688

**HAL Id: hal-00133688**

**<https://hal.science/hal-00133688>**

Submitted on 27 Feb 2007

**HAL** is a multi-disciplinary open access archive for the deposit and dissemination of scientific research documents, whether they are published or not. The documents may come from teaching and research institutions in France or abroad, or from public or private research centers.

L'archive ouverte pluridisciplinaire **HAL**, est destinée au dépôt et à la diffusion de documents scientifiques de niveau recherche, publiés ou non, émanant des établissements d'enseignement et de recherche français ou étrangers, des laboratoires publics ou privés.

# Coupling of Fast Multipole Method and Microlocal Discretization for the 3-D Helmholtz Equation

Eric DARRIGRAND

CEA/CESTA - MAB - LRC-M03, B.P.2, 33114 Le Barp, France

or

Université Bordeaux 1, Mathématiques Appliquées  
351 cours de la Libération, 33405 Talence Cedex, France  
E-mail: Eric.Darrigrand@math.u-bordeaux.fr

## Abstract

We are concerned with an integral method applied to the solution of the Helmholtz equation where the linear system is solved using an iterative method. We need to perform matrix-vector products whose time and memory requirements are increasing as a function of the wave number  $\kappa$ . A lot of methods have been developed in order to speed up the matrix-vector product calculation or to reduce the size of the system. Microlocal discretization methods enable one to consider new systems with reduced size. Another method, the fast multipole method, is one of the most efficient and robust methods used to speed up the calculation of matrix-vector products. In this paper, a coupling of these two recent methods is presented. It enables one to reduce the CPU time very efficiently for large wave numbers. Satisfactory numerical tests are also presented to confirm the theoretical study within a new integral formulation. Results are obtained for a sphere with a size of  $26\lambda$  by a resolution based on a mesh with an average edge length about  $2\lambda$  where  $\lambda$  is the wavelength.

## Key Words

Helmholtz, Integral Equation, Finite Element, Fast Multipole Method, Microlocal Discretization

## 1 Introduction

A numerical solution of the boundary integral equation for the exterior Helmholtz problem in three dimensions, leads to the solution of a dense linear system. In order to have a well conditioned system, we consider new integral equations written by B. Després. B. Després ([16], [31], see also [5] and [30]) wrote new integral equations with good properties that enable one to use an iterative solution based on the conjugate gradient. In order to accelerate the iterative solution of the system, we have considered a coupling of two methods, the microlocal discretization method and the fast multipole method (FMM).

With particular conditions, the microlocal discretization method, according to T. Abboud, J.-C. Nédélec and B. Zhou, consists in approximating the phase of the unknown using the geometrical optics method. Consequently, the oscillation of the new unknown is reduced. We can then consider a numerical approximation with a number of degrees of freedom  $N_d$  clearly less according to the wave number  $\kappa$ . Indeed, in the classical case we have  $N_d \sim \kappa^2$ , while  $N_d \sim \kappa^{2/3}$  after approximation of the phase. Nevertheless, the discretization of the geometry implies to consider  $\mathcal{O}(N)$  elements, with  $N \sim \kappa^2$ , on the surface of the obstacle. Then, the calculation of the matrix of the system also needs  $\mathcal{O}(N^2)$  operations with  $N \sim \kappa^2$ , as in the classical case. Thus, the authors of the method suggested the use of the theory of the stationary phase in order to accelerate the calculation of the matrix ([2]-[19]). However, this theory does not enable one to have a good estimate of the CPU time needed for a good

accuracy, and the extension to the 3-D case implies difficulties not yet solved. A. de la Bourdonnaye has also given another version of the microlocal discretization method ([15], [14]), making also use of the stationary phase theory.

The FMM is based on another idea. The issue is to factorize the product  $A.Y$  and to cluster advisedly the terms in order to reduce both resolution time and memory requirement. From the geometrical point of view, the calculus of far interactions is well speeded up by clustering the elements of the mesh properly. The one-level FMM (respectively multilevel FMM) results in an algorithm of complexity  $\mathcal{O}(N^{3/2})$  (respectively  $\mathcal{O}(N \ln^2 N)$ ) where  $N \sim \kappa^2$ . This method introduced for the Laplace equation by L. Greengard and V. Rokhlin ([17], [18]) was extended for the Helmholtz and Maxwell equations by V. Rokhlin ([25], [26]), W.C. Chew and co-authors ([33], [27], [7], [29], [28], [20]), E. Darve ([11], [12], [13]), and other authors ([8], [24]).

The object of this paper is to give a coupling of the microlocal discretization method according to T. Abboud, J.-C. Nédélec and B. Zhou, and the one-level FMM. The ideas of this work have briefly been presented for conferences ([9], [10]). Using the approximation of the phase of the unknown, the microlocal discretization method enables one to consider a numerical approximation with a number of degrees of freedom of order  $\kappa^{2/3}$  instead of  $\kappa^2$  in the classical case. The size of the system is then of order  $\kappa^{2/3} \times \kappa^{2/3}$ . Nevertheless, due to geometrical approximations, the matrix calculation still requires  $\mathcal{O}(\kappa^2 \times \kappa^2)$  operations. In this paper we suggest using the one-level FMM in order to speed up the matrix calculation instead of the theory of the stationary phase. This is a different use of the FMM since in our method the matrix of the system is calculated once and stored, and the FMM is used to accelerate its calculation. Thus, the matrix calculation is performed due to an algorithm with the complexity  $\kappa^3$  instead of  $\kappa^4$ . We also did a theoretical study of the use of a multilevel FMM. This should enable one to obtain a matrix calculation with the complexity  $\kappa^{8/3}$ . This idea will be the topic of a next paper.

First of all we give a presentation of the new integral equations and the classical solution of this system. Next, we present the microlocal discretization method and the FMM in order to give a comprehensive theoretical study of our coupling of both methods. Finally, numerical tests are considered to confirm the theoretical study. The scattering of the unit sphere is studied for large frequencies (up to a size of  $26\lambda$  and an area of  $2100\lambda^2$  for the sphere, with a coarse mesh whose average edge length is  $2\lambda$  where  $\lambda$  is the wavelength).

General notations:

$\imath$	$\sqrt{-1}$
$\lambda$	wavelength
$\kappa$	wave number $\kappa = 2\pi/\lambda$
$j_m$	spherical Bessel function
$y_m$	spherical Neumann function
$h_m^{(1)}$	spherical Hankel function of the first kind $h_m^{(1)} = j_m + \imath y_m$
$P_m$	Legendre polynomial
$S^2$	unit sphere $S^2 = \{\hat{s} \in \mathbb{R}^3 /  \hat{s}  = 1\}$

## 2 New Integral Equations for the 3-D Helmholtz Problem

### 2.1 Formulation of the new integral equations

B. Després wrote a new system of integral equations for the 3-D Maxwell equation and the 2-D Helmholtz equation. This system derives from the minimization of a quadratic functional. Classical systems do not have good matrix properties and are not suitable for an efficient iterative resolution. On the other hand, the considered IE (new integral equations according to B. Després) lead to a new system whose matrix properties enable one to use an efficient iterative resolution based on the conjugate gradient, without the use of preconditioning. Thus, in this paper, we study the coupling of the microlocal discretization and the fast multipole method for the solution of this IE system. However, this coupling could be considered in the same way for more classical integral systems. N. Bartoli and F. Collino rewrote the IE for the 2-D Helmholtz equation in a more comprehensible way (see [5]). In this section, we establish the IE for the 3-D Helmholtz equation in the similar way as N. Bartoli and F. Collino.

We first consider the Helmholtz equation with a particular impedance boundary condition

$$\begin{cases} \Delta u + \kappa^2 u = 0 , & \text{in } \Omega^+ , \\ \frac{\partial u}{\partial n} /_{\Gamma} + \imath \kappa u /_{\Gamma} = g , & \text{on } \Gamma , \\ \lim_{r \rightarrow +\infty} r \left( \frac{\partial u}{\partial r} - \imath \kappa u \right) = 0 , \end{cases} \quad (1)$$

where  $\Omega^-$  is a regular bounded domain of  $\mathbb{R}^3$ , of boundary  $\Gamma$ , and  $\Omega^+ = \mathbb{R}^3 \setminus \overline{\Omega^-}$  (Fig. 1).  $g$  is given as a function of the incident wave. The unit normal  $n$  is directed to the exterior domain.

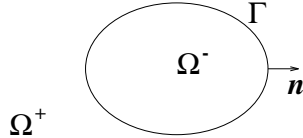


Figure 1: the obstacle

A first equation is obtained, considering that the solution of

$$\begin{cases} \Delta u + \kappa^2 u = 0 , & \text{in } \Omega^+ , \\ \lim_{r \rightarrow +\infty} r \left( \frac{\partial u}{\partial r} - \imath \kappa u \right) = 0 , \end{cases}$$

is given by

$$\kappa u = M(\kappa u /_{\Gamma}) - L\left(\frac{\partial u}{\partial n} /_{\Gamma}\right) \text{ in } \Omega^+ . \quad (2)$$

$L$  and  $M$  are the single and double-layer potential defined for all  $x$  not in  $\Gamma$  by

$$Lp(x) = \kappa \int_{\Gamma} G(x, y) p(y) d\gamma(y) \quad \text{and} \quad M\varphi(x) = \int_{\Gamma} \frac{\partial G}{\partial n_y}(x, y) \varphi(y) d\gamma(y)$$

$$\text{with } G(x, y) = \frac{e^{\imath\kappa|x-y|}}{4\pi|x-y|}.$$

With the notations  $q = \kappa u|_{\Gamma}$  and  $p = \frac{\partial u}{\partial n}|_{\Gamma}$ , we have the following relations

$$\begin{bmatrix} D & -K' - \frac{I}{2} \\ -K + \frac{I}{2} & S \end{bmatrix} \begin{bmatrix} q \\ p \end{bmatrix} = \begin{bmatrix} 0 \\ 0 \end{bmatrix} \quad (3)$$

where the operators  $S$ ,  $K$ ,  $K'$  and  $D$  are defined for all  $x$  in  $\Gamma$  by

$$\begin{aligned} Sp(x) &= \kappa \int_{\Gamma} G(x, y) p(y) d\gamma(y) \quad , & Dq(x) &= \frac{1}{\kappa} \int_{\Gamma} \frac{\partial^2 G}{\partial n_x \partial n_y}(x, y) q(y) d\gamma(y) \quad , \\ Kq(x) &= \int_{\Gamma} \frac{\partial G}{\partial n_y}(x, y) q(y) d\gamma(y) \quad , & K'p(x) &= \int_{\Gamma} \frac{\partial G}{\partial n_x}(x, y) p(y) d\gamma(y) \quad . \end{aligned}$$

The singularity of  $D$  will be treated by the following formula

$$\begin{aligned} \langle Dq, q' \rangle_{L^2(\Gamma)} &= \frac{1}{\kappa} \int_{\Gamma} \int_{\Gamma} G(x, y) [ \quad \kappa^2 q(y) \overline{q'(x)} (n_x \cdot n_y) \\ &\quad - \overrightarrow{\text{curl}}_{\Gamma} q(y) \cdot \overrightarrow{\text{curl}}_{\Gamma} \overline{q'(x)} \quad ] d\gamma(y) d\gamma(x) \quad . \end{aligned}$$

Considering the kernel expression, two other relations can be derived from the system (3). The kernel  $G(x, y)$  can be split into real and imaginary parts

$$G(x, y) = G_r(x, y) + \imath G_i(x, y) \quad , \quad \text{with} \quad \begin{cases} G_r(x, y) = \frac{\cos(\kappa|x-y|)}{4\pi|x-y|} \quad , \\ G_i(x, y) = \frac{\sin(\kappa|x-y|)}{4\pi|x-y|} \quad . \end{cases} \quad (4)$$

Following this decomposition, the operators read

$$S = S_r + \imath S_i \quad , \quad K = K_r + \imath K_i \quad , \quad K' = K'_r + \imath K'_i \quad , \quad D = D_r + \imath D_i$$

where  $S_r$ ,  $K_r$ ,  $K'_r$ ,  $D_r$ ,  $S_i$ ,  $K_i$ ,  $K'_i$  and  $D_i$  are real operators.

We now introduce a new couple of unknowns on the boundary,  $\mu = \imath q$  and  $\lambda = \imath p$ . Thus, the system (3) becomes

$$\mathbf{K} \begin{bmatrix} q \\ p \end{bmatrix} + \mathbf{M} \begin{bmatrix} \mu \\ \lambda \end{bmatrix} = \begin{bmatrix} 0 \\ 0 \end{bmatrix} \quad , \quad (5)$$

where

$$\mathbf{K} = \begin{bmatrix} D_r & -K'_r - \frac{I}{2} \\ -K_r + \frac{I}{2} & S_r \end{bmatrix} \quad \text{and} \quad \mathbf{M} = \begin{bmatrix} D_i & -K'_i \\ -K_i & S_i \end{bmatrix} ,$$

that implies, multiplying by  $\imath$

$$\mathbf{K} \begin{bmatrix} \mu \\ \lambda \end{bmatrix} = \mathbf{M} \begin{bmatrix} q \\ p \end{bmatrix} . \quad (6)$$

$S_r$  and  $D_r$  are symmetrical,  $\mathbf{K}$  is related to its adjoint  $\mathbf{K}^*$  through the relation

$$\mathbf{K} - \mathbf{K}^* = \begin{bmatrix} 0 & -I \\ I & 0 \end{bmatrix} = \Pi . \quad (7)$$

Up to now, the boundary condition has not been used. It implies the two equivalent relations

$$\begin{aligned} p + \mu &= g , \\ -\lambda + q &= -\imath g . \end{aligned}$$

Let  $\tilde{g} = \begin{bmatrix} -\imath g \\ g \end{bmatrix}$ , we obtain

$$\begin{bmatrix} q \\ p \end{bmatrix} + \Pi \begin{bmatrix} \mu \\ \lambda \end{bmatrix} = \tilde{g} . \quad (8)$$

Hence, considering the relations (8), (7) and (6), we obtain the following system

$$\begin{bmatrix} q \\ p \end{bmatrix} + \mathbf{M} \begin{bmatrix} q \\ p \end{bmatrix} - \mathbf{K}^* \begin{bmatrix} \mu \\ \lambda \end{bmatrix} = \tilde{g} . \quad (9)$$

We will now proceed to the derivation of the matrix  $\mathbf{M}$  from the far field operator in order to deduce some of its properties. Let us consider the operator defined for all  $p, q$  in  $L^2(\Gamma)$  and  $\hat{s}$  in  $S^2$  by

$$\left( A_\infty \begin{bmatrix} q \\ p \end{bmatrix} \right) (\hat{s}) = \frac{\kappa}{4\pi} \int_\Gamma e^{-\imath \kappa y \cdot \hat{s}} (p(y) + \imath (\hat{s} \cdot n_y) q(y)) d\gamma(y) . \quad (10)$$

Its adjoint is given for all  $\varphi$  in  $L^2(S^2)$  by

$$(A_\infty^* \varphi)(y) = \begin{bmatrix} \frac{-\kappa}{4\pi} \int_{S^2} \imath (\hat{s} \cdot n_y) e^{\imath \kappa y \cdot \hat{s}} \varphi(\hat{s}) d\hat{s} \\ \frac{\kappa}{4\pi} \int_{S^2} e^{\imath \kappa y \cdot \hat{s}} \varphi(\hat{s}) d\hat{s} \end{bmatrix} , \quad (11)$$

where  $\int_{S^2} d\hat{s}$  denotes the integral around the unit sphere  $S^2$ . Next, using the relation

$$\frac{\sin(\kappa|x-y|)}{4\pi|x-y|} = \frac{\kappa}{(4\pi)^2} \int_{S^2} e^{\imath \kappa(x-y) \cdot \hat{s}} d\hat{s} ,$$

we can easily check that

$$\mathbf{M} = A_\infty^* A_\infty , \quad (12)$$

i.e.  $\forall p, q \in L^2(\Gamma)$

$$\int_{S^2} A_\infty \begin{bmatrix} q \\ p \end{bmatrix} \cdot \overline{A_\infty \begin{bmatrix} \tilde{q} \\ \tilde{p} \end{bmatrix}} d\hat{s} = \int_\Gamma (\mathbf{M} \begin{bmatrix} q \\ p \end{bmatrix}) \cdot \overline{\begin{bmatrix} \tilde{q} \\ \tilde{p} \end{bmatrix}} d\Gamma . \quad (13)$$

Considering the relations (5) and (9), we obtain the following system

$$\begin{cases} X + A_\infty^* A_\infty X - \mathbf{K}^* Y = \tilde{g} , \\ \mathbf{K} X + A_\infty^* A_\infty Y = 0 , \end{cases} \quad (14)$$

where  $X = \begin{bmatrix} q \\ p \end{bmatrix}$  and  $Y = \imath X = \begin{bmatrix} \mu \\ \lambda \end{bmatrix}$ . The theory of the inf-sup condition enables one to check the existence and the unicity of  $X$  and the existence of  $Y$ . In order to gain the unicity of  $Y$ , B. Després suggested the following modification (see [5]), i.e. adding

$$\begin{aligned} & \beta X = -\imath \beta Y \quad \text{to the first equation} \\ \text{and} \quad & \beta Y = \imath \beta X \quad \text{to the second one,} \end{aligned} \quad (15)$$

given that  $\beta$  is a strictly positive parameter. We then obtain the  $\beta$ -system

$$\begin{cases} (Id + \beta) X + A_\infty^* A_\infty X - \mathbf{K}^* Y = \tilde{g} - \imath \beta Y , \\ \mathbf{K} X + (\beta + A_\infty^* A_\infty) Y = \imath \beta X . \end{cases} \quad (16)$$

Hence, the coercivity condition satisfied, the  $\beta$ -system has a unique solution  $(X, Y)$ .

Now, consider a general impedance condition, the Robin condition

$$\frac{\partial u}{\partial n} /_\Gamma + \imath \kappa Z u /_\Gamma = f \quad \text{on } \Gamma ,$$

where the impedance operator  $Z$  has a positive real part. The Dirichlet condition can be considered when  $Z \rightarrow +\infty$ . Let  $R$  be the associated reflection operator

$$R = \frac{Id - Z}{Id + Z} .$$

This condition is written in the form

$$\frac{\partial u}{\partial n} /_\Gamma + \imath \kappa u /_\Gamma = g \quad \text{on } \Gamma ,$$

with  $g$  expressed as follows

$$g = R(-\frac{\partial u}{\partial n} /_\Gamma + \imath \kappa u /_\Gamma) + (1 + R)f .$$

Thus, we can still have the system (16) with

$$\tilde{g} = \begin{bmatrix} -\imath g \\ g \end{bmatrix} = \begin{bmatrix} -\imath R(-p + \imath q) \\ R(-p + \imath q) \end{bmatrix} + \begin{bmatrix} -\imath(1+R)f \\ (1+R)f \end{bmatrix} .$$

Let  $F = \begin{bmatrix} -\imath(1+R)f \\ (1+R)f \end{bmatrix}$  and  $N_R = R \begin{bmatrix} 1 & \imath \\ \imath & -1 \end{bmatrix}$ , the system (16) is written

$$\begin{cases} (Id + \beta)X + A_\infty^* A_\infty X - \mathbf{K}^* Y = N_R X + F - \imath \beta Y , \\ \mathbf{K} X + (\beta + A_\infty^* A_\infty) Y = \imath \beta X . \end{cases} \quad (17)$$

i.e.

$$\mathcal{M}_\beta \begin{bmatrix} X \\ Y \end{bmatrix} = \mathcal{R}_{R,\beta} \begin{bmatrix} X \\ Y \end{bmatrix} + \begin{bmatrix} F \\ 0 \end{bmatrix} , \quad (18)$$

where

$$\mathcal{M}_\beta = \begin{bmatrix} (Id + \beta) + A_\infty^* A_\infty & -\mathbf{K}^* \\ \mathbf{K} & \beta + A_\infty^* A_\infty \end{bmatrix} \quad \text{and} \quad \mathcal{R}_{R,\beta} = \begin{bmatrix} N_R & -\imath \beta Id \\ \imath \beta Id & 0 \end{bmatrix} . \quad (19)$$

Due to the condition  $|R| \leq 1$ , the inf-sup condition is also satisfied in order to ensure existence and unicity of the solution.

We will now consider a finite element discretization of the system (17). Let  $\Gamma_h$  be an approximation of the surface  $\Gamma$ , obtained by a triangulation  $\mathcal{T}_h$ . Let  $V_h = \text{Vect}\{\varphi_i ; i = 1, N\}$  with  $\varphi_i, i \in \{1, \dots, N\}$  the  $\mathbb{P}_1$  basis functions associated to  $\mathcal{T}_h$ , and  $N$  the number of nodes of the finite element mesh  $\Gamma_h$ ,  $N \sim \kappa^2$

$$\varphi_i \in \mathbb{P}_1 \text{ and } \varphi_i(Nod_j) = \delta_{ij}$$

where  $Nod_j$  denotes the  $j^{\text{th}}$  node of the finite element mesh.

Let  $\psi_i = \begin{bmatrix} \varphi_i \\ 0 \end{bmatrix}$  and  $\psi_{i+N} = \begin{bmatrix} 0 \\ \varphi_i \end{bmatrix}$ , for all  $i$  in  $\{1, \dots, N\}$ .

After using the variational formulation, we obtain the following discrete system

$$\mathcal{M}_\beta \begin{bmatrix} X_h \\ Y_h \end{bmatrix} = \mathcal{R}_{R,\beta} \begin{bmatrix} X_h \\ Y_h \end{bmatrix} + \begin{bmatrix} F_h \\ 0 \end{bmatrix} , \quad (20)$$

where  $\mathcal{M}_\beta$  and  $\mathcal{R}_{R,\beta}$  are given by

$$\mathcal{M}_\beta = \begin{bmatrix} \mathcal{D}_\beta + \mathcal{A} & -\mathcal{K}^* \\ \mathcal{K} & \mathcal{B}_\beta + \mathcal{A} \end{bmatrix} \quad \text{and} \quad \mathcal{R}_{R,\beta} = \begin{bmatrix} \mathcal{N}_R & -\imath \mathcal{B}_\beta \\ \imath \mathcal{B}_\beta & 0 \end{bmatrix} , \quad (21)$$

with  $\mathcal{B}_\beta, \mathcal{D}_\beta, \mathcal{K}, \mathcal{K}^*, \mathcal{A}, \mathcal{N}_R$  the matrices  $2N \times 2N$  and  $F_h$  the vector of size  $2N$  defined by

$$\begin{aligned} (F_h)_j &= \langle F, \psi_j \rangle_{\mathbb{V}_h} , & (\mathcal{B}_\beta)_{ji} &= \langle \beta \psi_i, \psi_j \rangle_{\mathbb{V}_h} , \\ (\mathcal{D}_\beta)_{ji} &= \langle (1 + \beta) \psi_i, \psi_j \rangle_{\mathbb{V}_h} , & (\mathcal{N}_R)_{ji} &= \langle N_R \psi_i, \psi_j \rangle_{\mathbb{V}_h} , \\ (\mathcal{K})_{ji} &= \langle \mathbf{K} \psi_i, \psi_j \rangle_{\mathbb{V}_h} , & (\mathcal{K}^*)_{ji} &= \langle \mathbf{K}^* \psi_i, \psi_j \rangle_{\mathbb{V}_h} , \\ (\mathcal{A})_{ji} &= \langle A_\infty \psi_i, A_\infty \psi_j \rangle_{L^2(\mathcal{S}^2)} , & \text{or} & (\mathcal{A})_{ji} = \langle \mathbf{M} \psi_i, \psi_j \rangle_{\mathbb{V}_h} , \end{aligned} \quad (22)$$



where  $\mathbb{V}_h = V_h \times V_h$ . The discrete inf-sup condition also confirms the existence and unicity of the solution. The finite element structure ensures that the discrete solution converges to the solution to the continuous system (18).

## 2.2 Solution of the linear system

In order to solve the system (20), we suggest using the relaxed Jacobi method according to the following definition. Let  $\alpha$  be the relaxation parameter. Let  $\begin{bmatrix} X_h^{(0)} \\ Y_h^{(0)} \end{bmatrix}$  be such that  $Y_h^{(0)} = \imath X_h^{(0)}$ .

We define  $\left( \begin{bmatrix} X_h^{(n)} \\ Y_h^{(n)} \end{bmatrix} \right)_{n \geq 1}$  according to the relation

$$\begin{bmatrix} X_h^{(n)} \\ Y_h^{(n)} \end{bmatrix} = \alpha \begin{bmatrix} \tilde{X}_h^{(n)} \\ \tilde{Y}_h^{(n)} \end{bmatrix} + (1 - \alpha) \begin{bmatrix} X_h^{(n-1)} \\ Y_h^{(n-1)} \end{bmatrix} ,$$

where  $\begin{bmatrix} \tilde{X}_h^{(n)} \\ \tilde{Y}_h^{(n)} \end{bmatrix}$  is the solution of

$$\begin{bmatrix} \mathcal{D}_\beta + \mathcal{A} & -\mathcal{K}^* \\ \mathcal{K} & \mathcal{B}_\beta + \mathcal{A} \end{bmatrix} \begin{bmatrix} \tilde{X}_h^{(n)} \\ \tilde{Y}_h^{(n)} \end{bmatrix} = \begin{bmatrix} \mathcal{N}_R & -\imath \mathcal{B}_\beta \\ \imath \mathcal{B}_\beta & 0 \end{bmatrix} \begin{bmatrix} X_h^{(n-1)} \\ Y_h^{(n-1)} \end{bmatrix} + \begin{bmatrix} F_h \\ 0 \end{bmatrix} . \quad (23)$$

Let

$$\begin{bmatrix} V \\ W \end{bmatrix} = \begin{bmatrix} \mathcal{N}_R & -\imath \mathcal{B}_\beta \\ \imath \mathcal{B}_\beta & 0 \end{bmatrix} \begin{bmatrix} X_h^{(n-1)} \\ Y_h^{(n-1)} \end{bmatrix} + \begin{bmatrix} F_h \\ 0 \end{bmatrix} .$$

The  $n^{\text{th}}$  iteration of the solution boils down to the solution of the following system for  $\begin{bmatrix} X \\ Y \end{bmatrix}$

$$\begin{cases} (\mathcal{D}_\beta + \mathcal{A})X - \mathcal{K}^*Y = V \\ \mathcal{K}X + (\mathcal{B}_\beta + \mathcal{A})Y = W \end{cases} , \quad (24)$$

i.e.

$$\begin{cases} X = (\mathcal{D}_\beta + \mathcal{A})^{-1}(V + \mathcal{K}^*Y) \\ \mathcal{K}(\mathcal{D}_\beta + \mathcal{A})^{-1}V + \mathcal{K}(\mathcal{D}_\beta + \mathcal{A})^{-1}\mathcal{K}^*Y + (\mathcal{B}_\beta + \mathcal{A})Y = W \end{cases} . \quad (25)$$

Thus, the point at stake is to solve the following equation for  $Y$

$$(\mathcal{K}(\mathcal{D}_\beta + \mathcal{A})^{-1}\mathcal{K}^* + \mathcal{B}_\beta + \mathcal{A})Y = W - \mathcal{K}(\mathcal{D}_\beta + \mathcal{A})^{-1}V . \quad (26)$$

This solution is based on the use of the conjugate gradient method

1/ Calculation of  $Z = W - \mathcal{K}(\mathcal{D}_\beta + \mathcal{A})^{-1}V$

$\alpha$ ) Solution of  $(\mathcal{D}_\beta + \mathcal{A})\tilde{Z} = V$  according to the conjugate gradient method with the matrix  $(\mathcal{D}_\beta + \mathcal{A})$ .

$\beta$ )  $Z = W - \mathcal{K}\tilde{Z}$

2/ Solution of  $(\mathcal{K}(\mathcal{D}_\beta + \mathcal{A})^{-1}\mathcal{K}^* + \mathcal{B}_\beta + \mathcal{A})Y = Z$  using a conjugate gradient method with the matrix  $(\mathcal{K}(\mathcal{D}_\beta + \mathcal{A})^{-1}\mathcal{K}^* + \mathcal{B}_\beta + \mathcal{A})$ . In this way, we have to perform products of the form  $(\mathcal{D}_\beta + \mathcal{A})^{-1}\tilde{X}$  where  $\tilde{X}$  is a given vector. This kind of products is described in 1/  $\alpha$ ).

As far as the convergence of the conjugate gradient method is concerned, we can easily check that the matrices  $(\mathcal{D}_\beta + \mathcal{A})$  and  $(\mathcal{K}(\mathcal{D}_\beta + \mathcal{A})^{-1}\mathcal{K}^* + \mathcal{B}_\beta + \mathcal{A})$  are Hermitian positive definite. The convergence of the relaxed Jacobi method is ensured on the assumption that  $|R| < 1$ . Due to the integral operators  $\mathbf{K}$ ,  $\mathbf{K}^*$  and  $A_\infty$ , the calculation of the matrices  $\mathcal{K}$ ,  $\mathcal{K}^*$  and  $\mathcal{A}$  implies a calculus cost of order  $\mathcal{O}(N^2)$ . Regarding  $\mathcal{K}$  and  $\mathcal{K}^*$ , the calculation consists in performing the following expressions,  $\forall i, j \in \{1, \dots, N\}$

$$\begin{aligned}
1^\circ \quad & \langle S\varphi_i, \varphi_j \rangle_{V_h} = \kappa \int_{\Gamma_h} \int_{\Gamma_h} G(x, y) \varphi_i(y) \overline{\varphi_j(x)} d\gamma(y) d\gamma(x) \quad , \\
2^\circ \quad & \langle K\varphi_i, \varphi_j \rangle_{V_h} = \int_{\Gamma_h} \int_{\Gamma_h} \frac{\partial G}{\partial n_y}(x, y) \varphi_i(y) \overline{\varphi_j(x)} d\gamma(y) d\gamma(x) \quad , \\
3^\circ \quad & \langle K'\varphi_i, \varphi_j \rangle_{V_h} = \int_{\Gamma_h} \int_{\Gamma_h} \frac{\partial G}{\partial n_x}(x, y) \varphi_i(y) \overline{\varphi_j(x)} d\gamma(y) d\gamma(x) \quad , \\
4^\circ \quad & \langle D\varphi_i, \varphi_j \rangle_{V_h} = \frac{1}{\kappa} \int_{\Gamma_h} \int_{\Gamma_h} \frac{\partial^2 G}{\partial n_x \partial n_y}(x, y) \varphi_i(y) \overline{\varphi_j(x)} d\gamma(y) d\gamma(x) \quad .
\end{aligned} \tag{27}$$

The 4<sup>th</sup> term is performed according to the following formula ([23])

$$\begin{aligned}
\langle D\varphi_i, \varphi_j \rangle_{V_h} = \frac{1}{\kappa} \int_{\Gamma_h} \int_{\Gamma_h} G(x, y) [ & \kappa^2 \varphi_i(y) \overline{\varphi_j(x)} (n_x \cdot n_y) \\
& - \overrightarrow{\text{curl}}_{\Gamma_h} \varphi_i(y) \cdot \overrightarrow{\text{curl}}_{\Gamma_h} \overline{\varphi_j(x)} ] d\gamma(y) d\gamma(x) \quad .
\end{aligned}$$

Singularities for  $x = y$  are treated according to a change of variables in the close interactions. As regards  $\mathcal{A}$ , the calculation is performed using the relation  $(\mathcal{A})_{ji} = \langle A_\infty \psi_i, A_\infty \psi_j \rangle_{L^2(S^2)}$ .

Such a resolution has a complexity of order  $\mathcal{O}(N^2)$  due to the products matrix-vector with the matrices  $\mathcal{K}$ ,  $\mathcal{K}^*$  and  $\mathcal{A}$ . The next sections will then deal with speeding up the solution of the system (20).

### 3 Reduction of the Size of the System: Microlocal Discretization

In this section, we give a short presentation of the microlocal discretization method introduced by T. Abboud, J.-C. Nédélec and B. Zhou ([1], [2], [34]), assuming the following conditions to be met

- $\Omega$  is a bounded open *convex* domain in  $\mathbb{R}^3$ ,
- $u^{inc}$  is an incident *plane* wave.

Let  $q = u|_\Gamma$  be the potential on the boundary  $\Gamma$ . Let  $\Gamma_h$  be a piecewise  $l$ -degree polynomial boundary. We denote by  $\pi_h$  the orthogonal projection from  $\Gamma_h$  to  $\Gamma$ , which is a bijection if  $h$  is small

enough, where  $h$  denotes the greatest diameter of the elements of  $\Gamma_h$ . Consider  $q_h$  the unknown of the  $\mathbb{P}_m$  finite element discrete problem based on  $\Gamma_h$ , we then obtain the following estimates

$$\frac{\|q - \pi_h(q_h)\|_{H^s(\Gamma)}}{\|q\|_{H^s(\Gamma)}} \leq C (h\kappa)^{m+1}, \quad (28)$$

where  $s = 0$  in the Dirichlet case and  $s = 1/2$  in the Neumann case. These estimates involve the choice  $h \sim \kappa^{-1}$ . The method considered in this section permits to obtain new estimates using an approximation of the phase function of the unknown. It stems from the coupling of finite element methods and asymptotic methods. It involves concepts of asymptotic expansions of the amplitude and the phase functions introduced by the geometrical theory of diffraction and the uniformed theory of diffraction based on ray methods (see e.g. the book [6] by D. Bouche and F. Molinet). The unknown writes  $q = Qe^{i\phi}$  when  $Q$  is the amplitude and  $\phi$  the phase function. An asymptotic behaviour of the phase function is given by  $\phi = \kappa\phi_0 + \mathcal{O}(\kappa^{1/3})$  ([21], [32], [4]). An approximation of the phase function at the first degree is then given by  $\tilde{\phi} = \kappa\phi_0$ . When the obstacle is convex and the incident wave is plane, i.e.  $u^{inc}(x) = e^{i\kappa\xi \cdot x}$ ,  $\phi_0$  is defined by  $\phi_0(x) = \xi \cdot x$ . Denoting by  $\tilde{q}$  the new unknown such that  $q = \tilde{q}e^{i\kappa\phi_0}$ ,  $\tilde{q} = Qe^{i(\phi - \tilde{\phi})}$ , new error estimates are given as follows

$$\begin{aligned} \frac{\|\tilde{q} - \pi_h(\tilde{q}_h)\|_{L^2(\Gamma)}}{\|\tilde{q}\|_{L^2(\Gamma)}} &\leq C [h^m + h^l + (h\kappa^{1/3})^{m+1} + \kappa h^l] \\ &\text{in Dirichlet case,} \\ \frac{\|\tilde{q} - \pi_h(\tilde{q}_h)\|_{H^{1/2}(\Gamma)}}{\|\tilde{q}\|_{H^{1/2}(\Gamma)}} &\leq C [(h\kappa^{1/3})^{m+1} + \kappa^{3/2}h^l(\kappa h + 1)] \\ &\text{in Neumann and Robin cases.} \end{aligned} \quad (29)$$

The error associated to the boundary approximation consists of the  $h^l$  terms. On the other hand, the  $h^m$  terms come from the finite element discretization. Thus, thanks to the term  $h\kappa^{1/3}$ , a new mesh can be considered with  $h \sim \kappa^{-1/3}$ , but due to the terms  $\kappa h^l$  and  $\kappa^{3/2}h^l(\kappa h + 1)$ , we should consider a boundary approximation of degree  $l \geq 3$  in Dirichlet case and  $l \geq 7$  in Neumann and Robin cases. Such a consideration is very difficult to achieve numerically. Thus, T. Abboud, J.-C. Nédélec and B. Zhou proposed a new  $\mathbb{P}_m$  finite element method based on a coarse mesh  $\Gamma_c$  to define the unknown and a fine mesh  $\Gamma_f$  to approximate the boundary  $\Gamma$ .  $h_c$  and  $h_f$  will denote respectively the greatest diameter of the elements of  $\Gamma_c$  and of  $\Gamma_f$ . The unknown is defined on  $\Gamma_c$  and the integrals are performed on the fine mesh  $\Gamma_f$ . New error estimates are given by the following formulae

$$\begin{aligned} \frac{\|\tilde{q} - \pi_h(\tilde{q}_h)\|_{L^2(\Gamma)}}{\|\tilde{q}\|_{L^2(\Gamma)}} &\leq C [h_c^m + h_c^{-1}h_f^{l+1} + (h_c\kappa^{1/3})^{m+1} + \kappa h_c^{-1}h_f^{l+1}] \\ &\text{in Dirichlet case,} \\ \frac{\|\tilde{q} - \pi_h(\tilde{q}_h)\|_{H^{1/2}(\Gamma)}}{\|\tilde{q}\|_{H^{1/2}(\Gamma)}} &\leq C [\kappa^{1/2}h_c^{m+1/2} + \kappa^{1/2}h_f^{l+1} + (h_c\kappa^{1/3})^{m+1} + (h_f^l h_c^{-1} \kappa^{1/2} + \kappa^{3/2}h_f^l)(\kappa h_f + 1)] \\ &\text{in Neumann and Robin cases.} \end{aligned} \quad (30)$$

$\Gamma_c$  is associated to the discretization of the unknown with the  $h_c^m$  terms. The  $h_f^l$  terms confirm the contribution of  $\Gamma_f$  to the boundary discretization. These new error estimates imply the following

choices

$$h_c \sim \kappa^{-1/3} \quad , \quad h_f \sim \kappa^{-1} \quad (31)$$

In the Dirichlet case, we merely need a geometrical approximation with  $l = 1$ . In both Neumann and Robin cases,  $l \geq 3/2$  (then  $l \geq 2$ ) is a theoretical necessary condition, but the numerical tests show that the case  $l = 1$  is quite relevant.

Now, we have to introduce notations about the meshes. The unknown is defined from the coarse mesh  $\Gamma_c$ , with a number of nodes  $N_c$  of order  $\kappa^{2/3}$ .  $\Gamma_f$  denotes the fine mesh used to approach the surface of the obstacle, with a number of nodes  $N_f$  of order  $\kappa^2$ . Actually,  $\Gamma_f$  will be obtained from  $\Gamma_c$  as follows. We first consider  $\Gamma_c$  a given mesh. Let  $\Gamma_f^{-\pi}$  be the plane refinement of  $\Gamma_c$ . Then,  $\Gamma_f$  is obtained from  $\Gamma_f^{-\pi}$  by projection on the surface  $\Gamma$  of the obstacle. Due to these considerations, we subsequently denote by  $\pi$  the orthogonal projection from the plane triangles of  $\Gamma_c$  to the ones of  $\Gamma_f$ .  $\pi$  is such that  $\Gamma_f = \pi(\Gamma_f^{-\pi})$ . We also define  $\Gamma_c^s$  the projection of  $\Gamma_c$  on  $\Gamma_f$  by  $\pi$ . The elements of  $\Gamma_c^s$  follows the surface as  $\Gamma_f$  does, but are not plane elements.

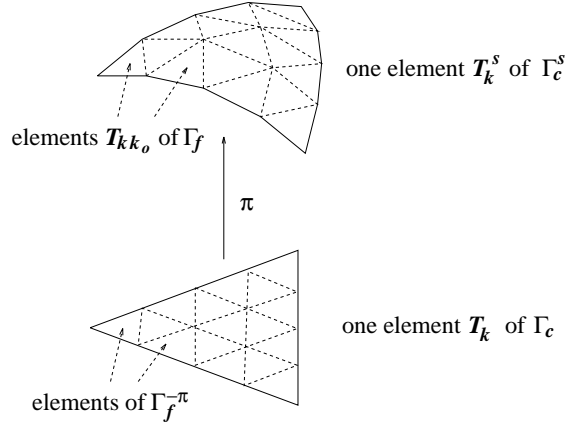


Figure 2: coarse mesh and fine mesh

In our case, we consider a new  $\mathbb{P}_1$  finite element discretization based on  $\Gamma_c^s$ . The new discrete space is then defined by

$$\tilde{V}_h(\Gamma_c^s) = \{ \tilde{q}_h / \tilde{q}_h = \tilde{q} \circ \pi^{-1}, \tilde{q}|_{T_j} \in \mathbb{P}_1(T_j) \} ,$$

where  $(T_j)_j$  describes the elements of  $\Gamma_c$ . To simplify the notations, the subscript  $h$  denotes  $h_c$ .

Let  $\psi_i = \begin{bmatrix} \varphi_i \\ 0 \end{bmatrix}$ ,  $\psi_{(i+N_c)} = \begin{bmatrix} 0 \\ \varphi_i \end{bmatrix}$ , for all  $i$  in  $\{1, \dots, N_c\}$ , where  $\varphi_i$ ,  $i \in 1, \dots, N_c$ , is the basis function associated to the  $i^{\text{th}}$  node of the mesh  $\Gamma_c$ . Let  $\tilde{\mathbb{V}}_h = \tilde{V}_h \times \tilde{V}_h$ .

The unknown is then given by  $q_h = \tilde{q}_h e^{i\kappa\phi_0} = \sum_{i=1}^{2N_c} \tilde{q}_i \tilde{\psi}_i$  and  $(\tilde{q}_i)_{i=1, \dots, 2N_c}$  is the new discrete unknown,

with  $\tilde{\psi}_i = (\psi_i \circ \pi^{-1}) e^{i\kappa\phi_0}$ .  $\psi_i$  is defined on  $\Gamma_c$  and evaluated only for points from the plane triangles of  $\Gamma_c$ , but the functions  $\tilde{\psi}_i$  and  $\phi_0$  are evaluated for quadrature points of the mesh  $\Gamma_c^s$ .

Hence, in our case defined in the previous section, the new system has a size of order  $N_c \times N_c$ . Using  $\tilde{\psi}_i$  like test functions, it can be written like (20)

$$\begin{bmatrix} \mathcal{D}_\beta + \mathcal{A} & -\mathcal{K}^* \\ \mathcal{K} & \mathcal{B}_\beta + \mathcal{A} \end{bmatrix} \begin{bmatrix} X_h \\ Y_h \end{bmatrix} = \begin{bmatrix} \mathcal{N}_R & -i\mathcal{B}_\beta \\ i\mathcal{B}_\beta & 0 \end{bmatrix} \begin{bmatrix} X_h \\ Y_h \end{bmatrix} + \begin{bmatrix} F_h \\ 0 \end{bmatrix}, \quad (32)$$

with the new definitions

$$\begin{aligned} (F_h)_j &= \langle F, \tilde{\psi}_j \rangle_{\tilde{\mathbb{V}}_h} = \langle F, (\psi_j \circ \pi^{-1}) e^{i\kappa\phi_0} \rangle_{\tilde{\mathbb{V}}_h}, \\ (\mathcal{B}_\beta)_{ji} &= \langle \beta \psi_i, \tilde{\psi}_j \rangle_{\tilde{\mathbb{V}}_h} = \langle \beta(\psi_i \circ \pi^{-1}) e^{i\kappa\phi_0}, (\psi_j \circ \pi^{-1}) e^{i\kappa\phi_0} \rangle_{\tilde{\mathbb{V}}_h}, \end{aligned} \quad (33)$$

and defined in the same way

$$\begin{aligned} (\mathcal{D}_\beta)_{ji} &= \langle (1 + \beta) \tilde{\psi}_i, \tilde{\psi}_j \rangle_{\tilde{\mathbb{V}}_h}, & (\mathcal{N}_R)_{ji} &= \langle N_R \tilde{\psi}_i, \tilde{\psi}_j \rangle_{\tilde{\mathbb{V}}_h}, \\ (\mathcal{K})_{ji} &= \langle \mathbf{K} \tilde{\psi}_i, \tilde{\psi}_j \rangle_{\tilde{\mathbb{V}}_h}, & (\mathcal{K}^*)_{ji} &= \langle \mathbf{K}^* \tilde{\psi}_i, \tilde{\psi}_j \rangle_{\tilde{\mathbb{V}}_h}, \\ (\mathcal{A})_{ji} &= \langle A_\infty \tilde{\psi}_i, A_\infty \tilde{\psi}_j \rangle_{L^2(S^2)}. \end{aligned} \quad (34)$$

For example, the duality  $\langle S\varphi_i, \varphi_j \rangle_{V_h}$  (27) becomes

$$\begin{aligned} \langle S\tilde{\varphi}_i, \tilde{\varphi}_j \rangle_{\tilde{\mathbb{V}}_h} &= \kappa \int_{\Gamma_c^s} \int_{\Gamma_c^s} G(x, y) \tilde{\varphi}_i(y) \overline{\tilde{\varphi}_j(x)} d\gamma(y) d\gamma(x), \\ &= \kappa \int_{\Gamma_f} \int_{\Gamma_f} G(x, y) \tilde{\varphi}_i(y) \overline{\tilde{\varphi}_j(x)} d\gamma(y) d\gamma(x), \\ &= \kappa \sum_{k/T_k^s \cap \text{supp}(\varphi_i) \neq \emptyset} \sum_{k_0} \sum_{l/T_l^s \cap \text{supp}(\varphi_j) \neq \emptyset} \sum_{l_0} \\ &\quad \int_{T_{k k_0}} \int_{T_{l l_0}} G(x, y) \varphi_i(\pi^{-1}(y)) e^{i\kappa\phi_0(y)} \overline{\varphi_j(\pi^{-1}(x)) e^{i\kappa\phi_0(x)}} d\gamma(y) d\gamma(x), \end{aligned} \quad (35)$$

where we denote by  $\{T_{k k_0}\}_{k_0}$  the set of triangles of  $\Gamma_f$  that make up  $T_k^s$  (see Fig. 2).

The new system (32) has the same properties as the previous one (20) due to the particular choice of the test functions. Thus, we select the same resolution, given in subsection 2.2.

Hence, we obtain a problem whose size is of order  $\kappa^{4/3}$  instead of  $\kappa^4$ . Thus, the memory cost is much less but, due to the performing of the matrices with respect to the consideration of the fine mesh  $\Gamma_f$ , the matrices calculation still requires  $\mathcal{O}(\kappa^4)$  operations. To reduce the cost, the authors T. Abboud, J.-C. Nédélec and B. Zhou, suggested using the theory of the stationary phase ([19]). However the numerical approach of this theory is very complicated and implies difficulties not yet solved in 3-D. In the next section we then present a study of the FMM in order to speed up the calculation of the matrices (see Section 5) without the theory of the stationary phase.

## 4 Acceleration of the Calculation: The One-Level Fast Multipole Method

The fast multipole method is a robust method that speeds up the calculation of the matrix-vector products of the iterative solution. We briefly present the one-level fast multipole method. For further information, we refer the reader to recent articles written by Darve for the multilevel FMM ([11], [12], [13]) and to previous articles ([8] or [27]).

The method is based on two developments. Through groups of elements, an uncoupling between two points is established using the Gegenbauer series and an integral around the unit sphere  $S^2$ . The obstacle is included inside a cube. Subdividing recursively the cube as an oct-tree, we obtain the groups of elements considering the boxes of the finest level.

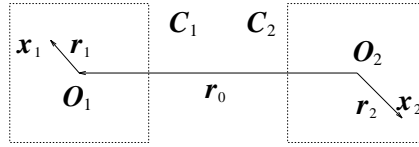


Figure 3: interaction between  $x_1$  and  $x_2$

Let  $x_1, x_2 \in \Gamma_h$ . Let  $O_1, O_2$  be the centers of the two boxes  $C_1$  and  $C_2$  including  $x_1$  and  $x_2$  (Fig. 3). Then,  $x_1 - x_2 = r_0 + r$  where  $r_0 = O_1 - O_2$ ,  $r = r_1 - r_2$  and  $r_i = x_i - O_i$ . With  $|r_0| > |r|$  the expansion of the Green function used by the multipole method is given by this formula (see [3])

$$\frac{e^{i\kappa|x_1-x_2|}}{4\pi|x_1-x_2|} \approx \frac{i\kappa}{(4\pi)^2} \sum_{p=1}^P \omega_p e^{i\kappa \langle s_p, r_1 \rangle} T_{L,r_0}(s_p) e^{-i\kappa \langle s_p, r_2 \rangle} \quad (36)$$

$$\text{with } T_{L,r_0}(s) = \sum_{m=0}^L (2m+1) i^m h_m^{(1)}(\kappa|r_0|) P_m(\cos(s, r_0)) .$$

The integer  $L$  is the truncation parameter of the Gegenbauer series and  $P$  the number of discrete directions  $\{s_p, p = 1, \dots, P\}$  corresponding to a numerical quadrature on the unit sphere  $S^2$ . The quadrature generally considered consists of a trapezoidal quadrature in the  $\varphi$  direction and a Gauss-Legendre quadrature in the  $\cos\theta$  direction where  $(\rho, \theta, \varphi)$  is the spherical coordinate system ([12], [20], [24]). Recent studies of Chew [20] validate the following empirical formula for  $L$ , for relatively large values of  $\kappa d$ :

$$L = \kappa d + C(\kappa d)^{1/3} , \quad (37)$$

where  $d$  is the diameter of the multipole boxes and  $C$  depends only on the desired accuracy. Next,  $P$  is given as follows

$$P = (L+1)(2L+1) . \quad (38)$$

We suggest the application of the one-level FMM to speed up the matrix-vector products whose matrix is, respectively,  $\mathcal{K}$ ,  $\mathcal{K}^*$  and  $\mathcal{A}$ , defined for the IE system in Section 2. New integral kernels and developments are considered here (see [22]). We have the following multipole approximation for the singular integral kernel of the IE system, when the matrix is  $\mathcal{K}$  or  $\mathcal{K}^*$  (see [3], p. 440)

$$\frac{\cos(\kappa|x_1 - x_2|)}{4\pi|x_1 - x_2|} \approx \frac{-\kappa}{(4\pi)^2} \sum_{p=1}^P \omega_p e^{i\kappa\langle s_p, r_1 \rangle} T_{L, r_0}^{\Re}(s_p) e^{-i\kappa\langle s_p, r_2 \rangle} \quad (39)$$

$$\text{with } T_{L, r_0}^{\Re}(s) = \sum_{m=0}^L (2m+1) i^m y_m(\kappa|r_0|) P_m(\cos(s, r_0)) .$$

The normal derivative of the integral kernel has the following approximation, for  $j = 1, 2$

$$\partial_{n_j} \frac{\cos(\kappa|x_1 - x_2|)}{4\pi|x_1 - x_2|} \approx \frac{(-1)^j i \kappa^2}{(4\pi)^2} \sum_{p=1}^P \omega_p \langle s_p, n(x_j) \rangle e^{i\kappa\langle s_p, r_1 \rangle} T_{L, r_0}^{\Re}(s_p) e^{-i\kappa\langle s_p, r_2 \rangle} . \quad (40)$$

After derivation,  $P$  must be a little greater than previously, as J. Rahola showed in [24]. As well as the classical case, the previous approximations are available for far interactions (condition  $|r_0| > |r|$ ).

We will now study the case of the matrix  $\mathcal{A}$ , with the regular integral kernel of the IE system. We then consider the relation  $(\mathcal{A})_{ji} = \langle \mathbf{M}\psi_i, \psi_j \rangle_{\mathbb{V}_h}$ . Due to the regularity of the integral kernel, the approximation can be written for all  $x_1, x_2$ . Thus, the far and close interactions are approximated in the same way

$$\frac{\sin(\kappa|x_1 - x_2|)}{4\pi|x_1 - x_2|} \approx \frac{\kappa}{(4\pi)^2} \sum_{p=1}^P \omega_p e^{i\kappa\langle s_p, r_1 \rangle} T_{L, r_0}^{\Im}(s_p) e^{-i\kappa\langle s_p, r_2 \rangle} \quad (41)$$

$$\text{with } T_{L, r_0}^{\Im}(s) = \sum_{m=0}^L (2m+1) i^m j_m(\kappa|r_0|) P_m(\cos(s, r_0)) .$$

The normal derivative of the integral kernel has the following approximation, for  $j = 1, 2$

$$\partial_{n_j} \frac{\sin(\kappa|x_1 - x_2|)}{4\pi|x_1 - x_2|} \approx \frac{(-1)^{j+1} i \kappa^2}{(4\pi)^2} \sum_{p=1}^P \omega_p \langle s_p, n(x_j) \rangle e^{i\kappa\langle s_p, r_1 \rangle} T_{L, r_0}^{\Im}(s_p) e^{-i\kappa\langle s_p, r_2 \rangle} , \quad (42)$$

$$\partial_{n_1} \partial_{n_2} \frac{\sin(\kappa|x_1 - x_2|)}{4\pi|x_1 - x_2|} \approx \frac{\kappa^3}{(4\pi)^2} \sum_{p=1}^P \omega_p \langle s_p, n(x_1) \rangle \langle s_p, n(x_2) \rangle e^{i\kappa\langle s_p, r_1 \rangle} T_{L, r_0}^{\Im}(s_p) e^{-i\kappa\langle s_p, r_2 \rangle} . \quad (43)$$

We give for example the algorithm of the fast product  $\mathcal{M}Y$  for a given vector  $Y$  and with the matrix  $\mathcal{M}$  defined by

$$\forall i, j \in \{1, \dots, N\} , \quad \mathcal{M}_{ij} = \overline{\alpha_i} \alpha_j G_r(\kappa, |x_i - x_j|) , \quad \alpha_i , \alpha_j \in \mathbb{C} ,$$

The matrix stands for a discretization of (27-1°). We apply the one-level FMM using the relation (39). Let  $N_{fmm}$  be the number of FMM boxes. Due to the condition  $|r_0| > |r|$ , we consider the close part and the far part of the matrix, for  $x_i$  in a FMM box  $C$  and  $x_j$  in a FMM box  $\tilde{C}$

$$(\mathcal{M}^{far})_{ij} = \begin{cases} 0 & \text{if } \tilde{C} \text{ close to } C \\ \mathcal{M}_{ij} & \text{if } \tilde{C} \text{ far from } C \end{cases}, \quad (\mathcal{M}^{close})_{ij} = \begin{cases} \mathcal{M}_{ij} & \text{if } \tilde{C} \text{ close to } C \\ 0 & \text{if } \tilde{C} \text{ far from } C \end{cases}, \quad (44)$$

where “ $\tilde{C}$  close to  $C$ ” means that the cubes  $\tilde{C}$  and  $C$  have at least one common vertex. The multipole approximation is given by the following relation, for all  $i$  in  $\{1, \dots, N\}$ ,  $x_i$  in a box  $C$

$$(\mathcal{M}^{far} Y)_i \approx \Psi_i \equiv \frac{-\kappa}{(4\pi)^2} \bar{\alpha}_i \sum_{p=1}^P \omega_p e^{i\kappa \langle s_p, r_i \rangle} \sum_{\tilde{C} \text{ far from } C} T_{L, r_{C\tilde{C}}}^{\Re}(s_p) \sum_{j/x_j \in \tilde{C}} e^{-i\kappa \langle s_p, r_j \rangle} \alpha_j Y_j. \quad (45)$$

Thus, the algorithm of the calculation of the matrix-vector product  $\mathcal{M}^{far} Y$ , using the one-level FMM, consists of four steps (Fig. 4)

*Step 1:* Transfer functions: Translation between two boxes  $T_{L, O_C - O_{\tilde{C}}}^{\Re}(s_p)$  defined in (39),

$\forall (O_C - O_{\tilde{C}})$ , with  $C$  and  $\tilde{C}$  two far FMM boxes,  $\forall p \in \{1, \dots, P\}$ .

*Step 2:* Radiation functions:  $\forall \tilde{C}$  FMM box,  $\forall p \in \{1, \dots, P\}$

$$F_{\tilde{C}}(s_p) = \sum_{j/x_j \in \tilde{C}} e^{i\kappa \langle s_p, O_{\tilde{C}} - x_j \rangle} \alpha_j Y_j.$$

*Step 3:* Transfer from  $\tilde{C}$  to  $C$ :  $\forall C$  FMM box,  $\forall p \in \{1, \dots, P\}$

$$G_C(s_p) = \sum_{\tilde{C} \text{ far from } C} T_{L, O_C - O_{\tilde{C}}}^{\Re}(s_p) F_{\tilde{C}}(s_p).$$

*Step 4:* Integration on  $S^2$ :  $\forall i \in \{1, \dots, N\}$ ,  $x_i \in C$  FMM box

$$\Psi_i = \frac{-\kappa}{(4\pi)^2} \bar{\alpha}_i \sum_{p=1}^P \omega_p e^{i\kappa \langle s_p, x_i - O_C \rangle} G_C(s_p).$$

The other discrete calculations of the products with the matrices  $\mathcal{K}$  and  $\mathcal{K}^*$  are performed in the same way, using the relations (39) and (40). We mean also to calculate products with  $\mathcal{A}$  in the same way, using the relations (41), (42) and (43). Moreover, this matrix enables us to perform close interactions as well as far ones.

Choosing a number of FMM boxes  $N_{fmm} \sim N^{1/2}$ , we obtain an algorithm with the complexity  $\mathcal{O}(N^{3/2})$ , i.e.  $\mathcal{O}(\kappa^3)$  ([8]).



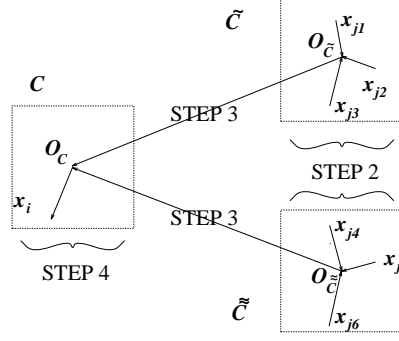


Figure 4: far interactions

## 5 Coupling: Microlocal Discretization and Fast Multipole Method

The coupling is based on the reduction of the size of the system using the approximation of the phase function, and the acceleration of the matrix calculation using the one-level FMM. The one-level FMM is considered instead of the theory of the stationary phase. The matrix-vector product is then performed in a classical way. Due to the approximation of the phase function, we have to consider the coarse mesh (introduced in Section 3). The unknown is defined on the coarse mesh and, in order to have a good geometrical approximation of  $\Gamma$ , we resort to the fine mesh which is used in classical methods. For the multipole method, the elements of the fine mesh are grouped in boxes (Fig. 5).

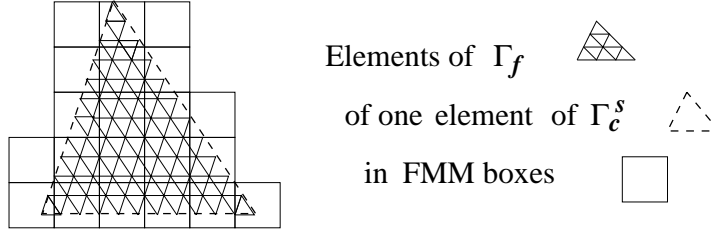


Figure 5: meshes and FMM boxes

Then, we consider the approximation of the phase function given by the microlocal discretization. Using notations of Section 3, we consider the same system (32)-(33)-(34).

$$\begin{bmatrix} \mathcal{D}_\beta + \mathcal{A} & -\mathcal{K}^* \\ \mathcal{K} & \mathcal{B}_\beta + \mathcal{A} \end{bmatrix} \begin{bmatrix} X_h \\ Y_h \end{bmatrix} = \begin{bmatrix} \mathcal{N}_R & -\imath \mathcal{B}_\beta \\ \imath \mathcal{B}_\beta & 0 \end{bmatrix} \begin{bmatrix} X_h \\ Y_h \end{bmatrix} + \begin{bmatrix} F_h \\ 0 \end{bmatrix}, \quad (46)$$

with the definitions

$$(F_h)_j = \langle F, \tilde{\psi}_j \rangle_{\tilde{\mathbb{V}}_h} = \langle F, (\psi_j \circ \pi^{-1}) e^{\imath \kappa \phi_0} \rangle_{\tilde{\mathbb{V}}_h}, \quad (47)$$

$$(\mathcal{B}_\beta)_{ji} = \langle \beta \tilde{\psi}_i, \tilde{\psi}_j \rangle_{\tilde{\mathbb{V}}_h} = \langle \beta (\psi_i \circ \pi^{-1}) e^{\imath \kappa \phi_0}, (\psi_j \circ \pi^{-1}) e^{\imath \kappa \phi_0} \rangle_{\tilde{\mathbb{V}}_h}, \quad (48)$$

in the same way

$$(\mathcal{D}_\beta)_{ji} = \langle (1 + \beta) \tilde{\psi}_i, \tilde{\psi}_j \rangle_{\tilde{\mathbb{V}}_h} , \quad (\mathcal{N}_R)_{ji} = \langle N_R \tilde{\psi}_i, \tilde{\psi}_j \rangle_{\tilde{\mathbb{V}}_h} , \quad (49)$$

$$(\mathcal{K})_{ji} = \langle \mathbf{K} \tilde{\psi}_i, \tilde{\psi}_j \rangle_{\tilde{\mathbb{V}}_h} , \quad (\mathcal{K}^*)_{ji} = \langle \mathbf{K}^* \tilde{\psi}_i, \tilde{\psi}_j \rangle_{\tilde{\mathbb{V}}_h} , \quad (50)$$

$$(\mathcal{A})_{ji} = \langle \mathbf{M} \tilde{\psi}_i, \tilde{\psi}_j \rangle_{\tilde{\mathbb{V}}_h} . \quad (51)$$

The matrices  $\mathcal{B}_\beta$ ,  $\mathcal{D}_\beta$  and  $\mathcal{N}_R$  are performed in a classical way with  $\mathcal{O}(N_f)$  operations. In order to speed up the calculation of the matrices  $\mathcal{K}$ ,  $\mathcal{K}^*$  and  $\mathcal{A}$ , we use the one-level FMM instead of the stationary phase, as described below. We recall that  $\{T_{k\ k_0}\}_{k_0}$  is the set of triangles of  $\Gamma_f$  that make up  $T_k^s$ . Let us consider the matrix  $\mathcal{M}$  defined as follows,  $\forall i, j \in \{1, \dots, N_c\}$  :

$$\mathcal{M}_{ij} = \sum_{k/T_k^s \cap \text{supp}(\varphi_i) \neq \emptyset} \sum_{l/T_l^s \cap \text{supp}(\varphi_j) \neq \emptyset} \sum_{T_{k\ k_0}} \sum_{T_{l\ l_0}} \overline{\alpha_{k\ k_0}} \overline{e^{i\kappa\phi_0(x_{k\ k_0})}} \alpha_{l\ l_0} e^{i\kappa\phi_0(x_{l\ l_0})} G_r(\kappa, |x_{k\ k_0} - x_{l\ l_0}|) ,$$

with  $\alpha_{k\ k_0}, \alpha_{l\ l_0} \in \mathbb{C}$ .

The matrix stands for a discretization of (27-1°) with our new definitions (50). We apply the one-level FMM separating the close part from the far part of the matrix, and using the relation (39). Thus, the multipole approximation is given by

$$\begin{aligned} \forall i, j \in \{1, \dots, N_c\} \\ (\mathcal{M}_{approx}^{far})_{ij} = \frac{-\kappa}{(4\pi)^2} \sum_{p=1}^P \omega_p \sum_{k/T_k^s \cap \text{supp}(\varphi_i) \neq \emptyset} \sum_{C/T_k^s \cap C \neq \emptyset} \sum_{k_0/x_{k\ k_0} \in C} \overline{\alpha_{k\ k_0}} \overline{e^{i\kappa\phi_0(x_{k\ k_0})}} e^{i\kappa \langle s_p, r_{k\ k_0} \rangle} \\ \times \sum_{l/T_l^s \cap \text{supp}(\varphi_j) \neq \emptyset} \sum_{\substack{\tilde{C}/T_l^s \cap \tilde{C} \neq \emptyset \\ \tilde{C} \text{ far from } C}} T_{L, r_{C\tilde{C}}}^{\Re}(s_p) \sum_{l_0/x_{l\ l_0} \in \tilde{C}} \alpha_{l\ l_0} e^{i\kappa\phi_0(x_{l\ l_0})} e^{-i\kappa \langle s_p, r_{l\ l_0} \rangle} , \end{aligned} \quad (52)$$

with  $L$  and  $P$  defined by (37) and (38). Hence, the algorithm of the calculation of the matrix  $\mathcal{M}^{far}$ , using the one-level FMM, consists of three steps:

*Step 1:* Tansfer functions:  $\forall (O_C - O_{\tilde{C}}), \tilde{C}$  far from  $C, \forall p \in \{1, \dots, P\}$

$$T_{L, O_C - O_{\tilde{C}}}^{\Re}(s_p) = \sum_{m=0}^L (2m+1) i^m y_m(\kappa |O_C - O_{\tilde{C}}|) P_m(\cos(s_p, O_C - O_{\tilde{C}})) .$$

*Step 2:* New radiation functions:  $\forall i \in \{1, \dots, N_c\}, \forall k/T_k^s \cap \text{supp}(\varphi_i) \neq \emptyset, \forall C$  FMM box such that  $T_k^s \cap C \neq \emptyset, \forall p \in \{1, \dots, P\}$

$$F_{k\ C}(s_p) = \sum_{k_0/x_{k\ k_0} \in C} \alpha_{k\ k_0} e^{i\kappa\phi_0(x_{k\ k_0})} e^{i\kappa \langle s_p, O_C - x_{k\ k_0} \rangle} .$$

Step 3: Approximation of the matrix,  $\forall i, j \in \{1, \dots, N_c\}$

$$(\mathcal{M}_{approx}^{far})_{ij} = \frac{-\kappa}{(4\pi)^2} \sum_{p=1}^P \omega_p \sum_{k/T_k^s \cap \text{supp}(\varphi_i) \neq \emptyset} \sum_{C/T_k^s \cap C \neq \emptyset} \overline{F_{kC}(s_p)} \\ \sum_{l/T_l^s \cap \text{supp}(\varphi_j) \neq \emptyset} \sum_{\substack{\tilde{C}/T_l^s \cap \tilde{C} \neq \emptyset \\ \tilde{C} \text{ far from } C}} T_{L, O_C - O_{\tilde{C}}}^{\Re}(s_p) F_{l\tilde{C}}(s_p) .$$

Then, a matrix-vector product with the matrix  $\mathcal{M}$  is approximated by the following calculation,  $\forall i \in \{1, \dots, N_c\}$

$$(\mathcal{M}Y)_i = \sum_{j=1}^{N_c} ((\mathcal{M}^{close})_{ij} + (\mathcal{M}_{approx}^{far})_{ij}) Y_j ,$$

where  $\mathcal{M}^{close}$  is performed in a classical way.

The other discrete calculations of the matrices  $\mathcal{K}$  and  $\mathcal{K}^*$  are performed in the same way, using the relations (39) and (40). The relations (41), (42) and (43) enable one to perform a multipole approximation of the matrix  $\mathcal{A}$ . Denoting by  $N_{fmm}$  the number of FMM boxes, the new theoretical complexity of the calculation cost is given for a product  $\mathcal{M}Y$  in the following table, where  $\mathcal{M}$  is one of the matrices  $\mathcal{K}$ ,  $\mathcal{K}^*$  and  $\mathcal{A}$

	Independent of $Y$	Dependent on $Y$
$\mathcal{M}^{far}$	$\sim 8LN_f + \frac{N_f^2}{N_{fmm}} + \max(N_{fmm}^2, N_c^2) \frac{N_f}{N_{fmm}}$	$\sim N_c^2$
$\mathcal{M}^{close}$	$\sim \frac{N_f^2}{N_{fmm}}$	$\sim N_c^2$

The memory cost has the complexity  $\mathcal{O}\left(\max(N_{fmm}, N_c) \frac{N_f}{N_{fmm}} + N_c^2\right)$ .

Concerning the number of FMM boxes, the optimal choice is then  $N_{fmm} \sim N_f^{1/2}$ . Thus, the number of FMM boxes,  $N_{fmm}$  is greater than  $N_c$ . Now, we can compare the different methods

	Calculation independent of $Y$	Calculation dependent on $Y$	Memory
Microlocal Discretization without stationary phase	$\sim N_f^2$	$\sim N_f^{2/3}$	$\sim N_f$
1 Level FMM ( $N_{fmm} \sim N_f^{1/2}$ )	$\sim N_f^{5/4}$ ( or $N_f^{3/2}$ )	$\sim N_f^{3/2}$	$\sim N_f$ ( or $N_f^{3/2}$ )
New Method ( $N_{fmm} \sim N_f^{1/2}$ )	$\sim N_f^{3/2}$	$\sim N_f^{2/3}$	$\sim N_f$

With our new method, the calculation which is independent of  $Y$  corresponds to the matrix calculation and is performed once. On the other hand, the calculation that is dependent on  $Y$  is performed to each iteration. Let  $N_{iter}$  be the number of iterations within the iterative solution of the system. The global CPU time of our new method is then  $\mathcal{O}(N_f^{3/2} + N_{iter} N_f^{2/3})$ . With the one-level FMM, users classically store the part of the matrix corresponding to the close interactions that are performed once. That implies the complexity given between brackets. However, in order to consider industrial test cases, we do not store the close part of the matrix and we perform them to each iteration. Hence, our one-level FMM has a CPU time of complexity  $\mathcal{O}(N_f^{5/4} + N_{iter} N_f^{3/2})$  and requires a storage of complexity  $\mathcal{O}(N_f)$ . Anyway, our method appears really more efficient than the one-level FMM for all  $N_{iter}$ . Moreover, due to the difficulties of the theory of the stationary phase in 3-D, our new method is more robust than the microlocal discretization with stationary phase and obviously more efficient than the microlocal discretization without stationary phase.

## 6 Numerical Results

In order to validate the new method, four codes were written. The first one denoted by  $\mathcal{C}(\text{IE})$  solves the IE system in a classical way as defined in Section 2. The second code,  $\mathcal{C}(\text{IE}+\text{FMM})$  is a variant of the previous one, speeding up the matrix-vector products using the one-level FMM as explained in Section 4. The third one,  $\mathcal{C}(\text{IE}+\text{MD})$  is an application of the microlocal discretization method to the IE system, as explained in Section 3. The code  $\mathcal{C}(\text{IE}+\text{MD}+\text{FMM})$  is an application of the coupling of both microlocal discretization and one-level FMM to the IE system which we achieved in Section 5. As regards the IE system, the parameter  $\beta$  of the  $\beta$ -system (16) is chosen equal to 0.5. The relaxation parameter of the relaxed Jacobi method is set equal to 0.7 (see Subsection 2.2). Concerning the FMM, the number of terms in the Gegenbauer series defined by  $L = \kappa d + C(\kappa d)^{1/3}$  (see Section 4) is evaluated with  $C = 6$  and  $d$  the diameter of the multipole boxes. Besides, we denote by JM the Jacobi method, GC1 the conjugate gradient applied to the matrix  $(\mathcal{D}_\beta + \mathcal{A})$  (see Subsection 2.2) and GC2 the second conjugate gradient. In this section, we also denote by  $N_f$ ,  $N_c$  and  $N_{fmm}$ , the number of triangles of  $\Gamma_f$ , the number of triangles of  $\Gamma_c$  and the number of FMM boxes. All the results are obtained on a processor EV67 on a Compaq cluster ES40.

We present numerical tests for the unit sphere with a diameter  $D = 2$  which make it possible to compare numerical solutions with the exact solution, the Mie series solution. Comparisons are made considering the bistatic RCS (Radar Cross Section). The results are obtained with the residual  $10^{-4}$  and  $10^{-3}$  respectively for GC1 and GC2, and the difference  $10^{-3}$  between two iterates of JM. With the sphere, we consider a plane incident wave of direction  $(0, 0, -1)$ . Fig. 6 validates  $\mathcal{C}(\text{IE})$  and the FMM contribution in  $\mathcal{C}(\text{IE}+\text{FMM})$ . Regarding CPU time and memory requirements, we can give the gain which results from the FMM approximation. Concerning the accuracy, the following table shows the good behaviour of the FMM.  $Err(AD)$  denotes the relative error in  $l^2$ -average made on the diffusion amplitude in comparison with the Mie series solution. Let  $Y_{\imath X}$  be the relative error  $\frac{\|Y_h - \imath X_h\|_2}{\|X_h\|_2}$ .

		CPU time (min)	Memory	$Y_{\mathcal{I}X}$	$Err(AD)$
Fig. 6 a)	$\mathcal{C}(\text{IE})$	15256	682 MB	$2.3 \cdot 10^{-3}$	$0.6 \cdot 10^{-4}$
	$\mathcal{C}(\text{IE}+\text{FMM})$	6048	522 MB	$9.1 \cdot 10^{-3}$	$1.3 \cdot 10^{-4}$
Fig. 6 b)	$\mathcal{C}(\text{IE})$	11311	682 MB	$3.8 \cdot 10^{-3}$	$0.4 \cdot 10^{-3}$
	$\mathcal{C}(\text{IE}+\text{FMM})$	546	521 MB	$8.9 \cdot 10^{-3}$	$1.5 \cdot 10^{-3}$
Fig. 6 c)	$\mathcal{C}(\text{IE})$	17701	682 MB	$3.1 \cdot 10^{-3}$	$0.5 \cdot 10^{-3}$
	$\mathcal{C}(\text{IE}+\text{FMM})$	8450	522 MB	$9.4 \cdot 10^{-3}$	$0.6 \cdot 10^{-3}$

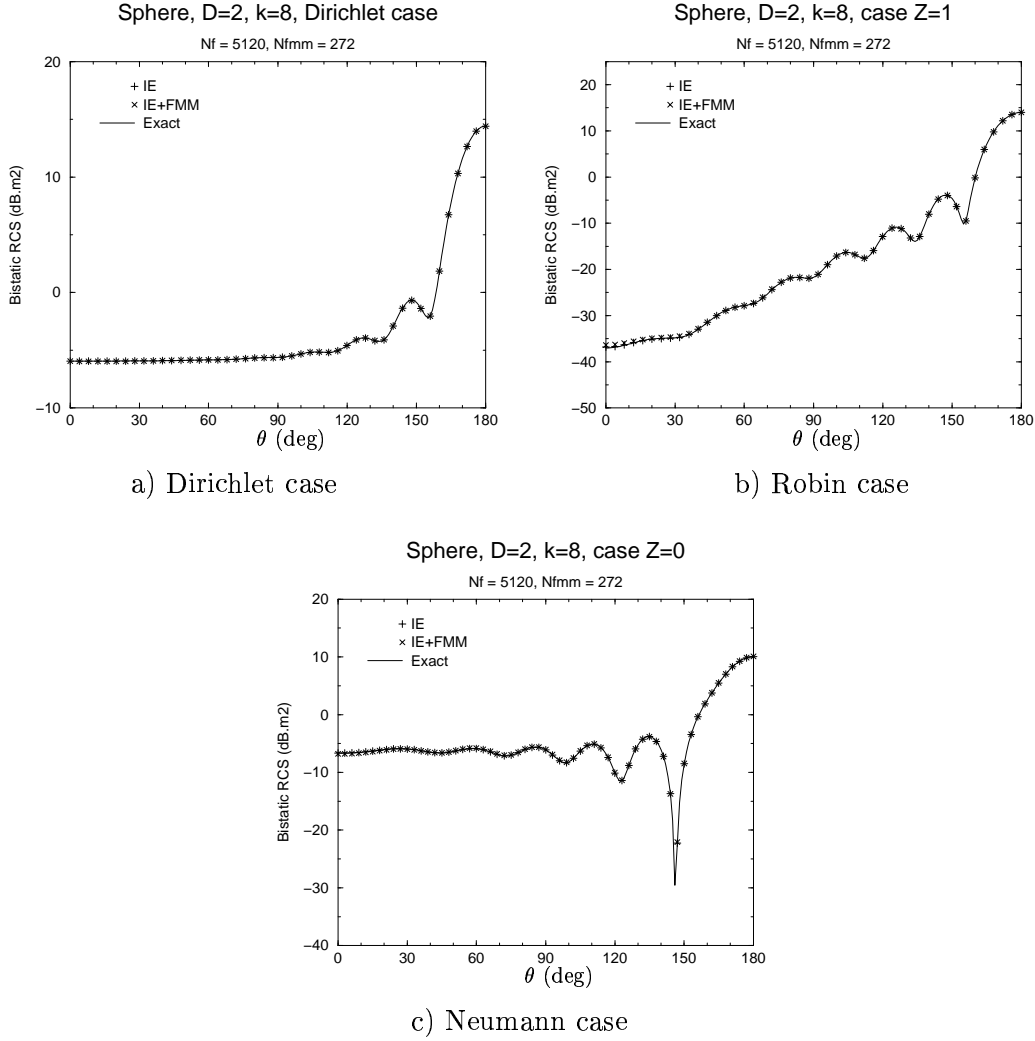


Figure 6:  $\mathcal{C}(\text{IE}) - \mathcal{C}(\text{IE}+\text{FMM})$ , for  $\kappa = 8$

In the same way, Fig. 7 validates the FMM contribution in  $\mathcal{C}(\text{IE}+\text{MD}+\text{FMM})$ .

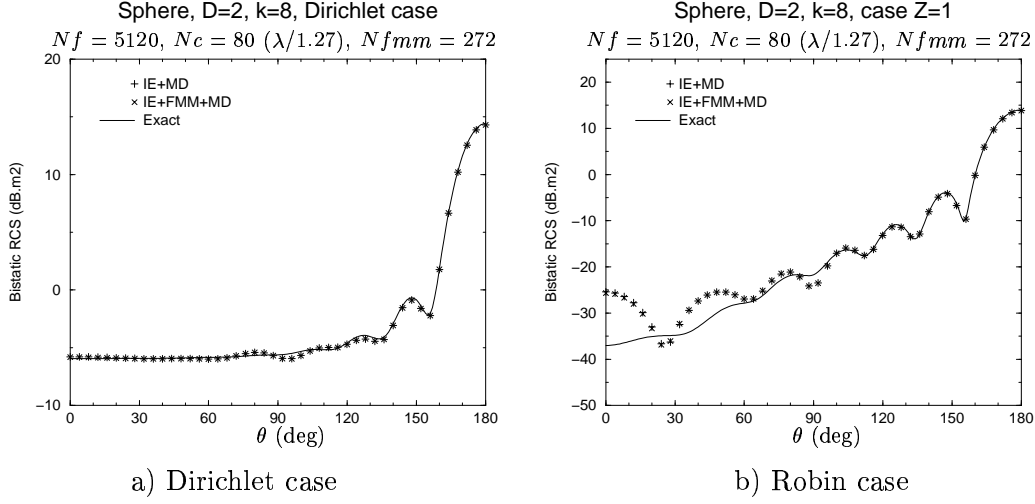


Figure 7:  $\mathcal{C}(\text{IE}+\text{MD}) - \mathcal{C}(\text{IE}+\text{MD}+\text{FMM})$ , for  $\kappa = 8$

We can also give the gain which results from the FMM approximation and the accuracy of the different tests in the following table.

		CPU time (min)	Memory	$Y_i X$	$Err(AD)$
Fig. 7 a)	$\mathcal{C}(\text{IE}+\text{MD})$	1613	12 MB	$1.2 \cdot 10^{-2}$	$1.5 \cdot 10^{-3}$
	$\mathcal{C}(\text{IE}+\text{MD}+\text{FMM})$	183	37 MB	$1.3 \cdot 10^{-2}$	$1.5 \cdot 10^{-3}$
Fig. 7 b)	$\mathcal{C}(\text{IE}+\text{MD})$	1599	12 MB	$2.5 \cdot 10^{-2}$	$5.3 \cdot 10^{-2}$
	$\mathcal{C}(\text{IE}+\text{MD}+\text{FMM})$	181	37 MB	$2.6 \cdot 10^{-2}$	$5.1 \cdot 10^{-2}$

Thus, thanks to the good behaviour of the FMM approximation, the contribution of the microlocal discretization, i.e. the code  $\mathcal{C}(\text{IE}+\text{MD})$ , is validated by the validation of the code  $\mathcal{C}(\text{IE}+\text{MD}+\text{FMM})$  which follows.

We now validate the code  $\mathcal{C}(\text{IE}+\text{MD}+\text{FMM})$  considering frequencies higher and higher with the sphere. The following figures (Fig. 8 and Fig. 9) show excellent results obtained for the Dirichlet boundary condition.

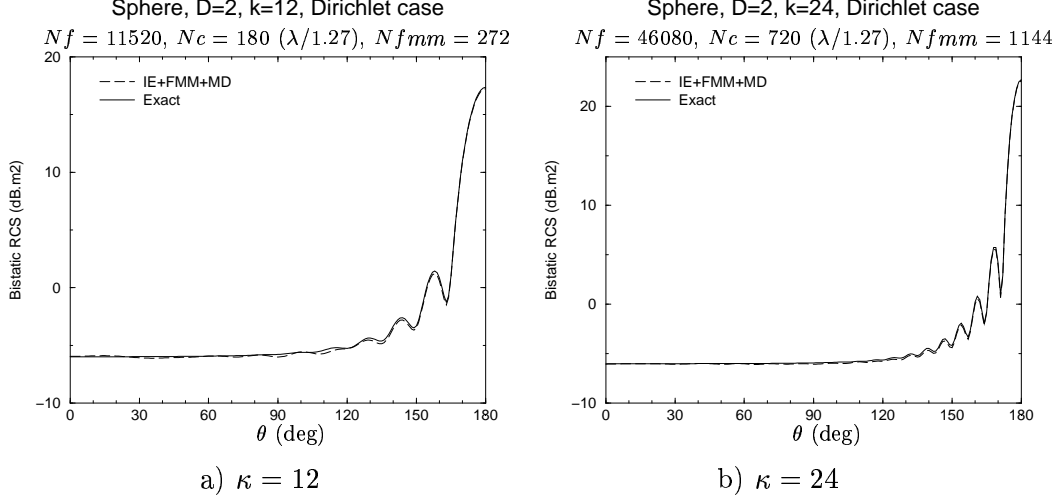


Figure 8:  $\mathcal{C}(\text{IE}+\text{MD}+\text{FMM})$ , Dirichlet case

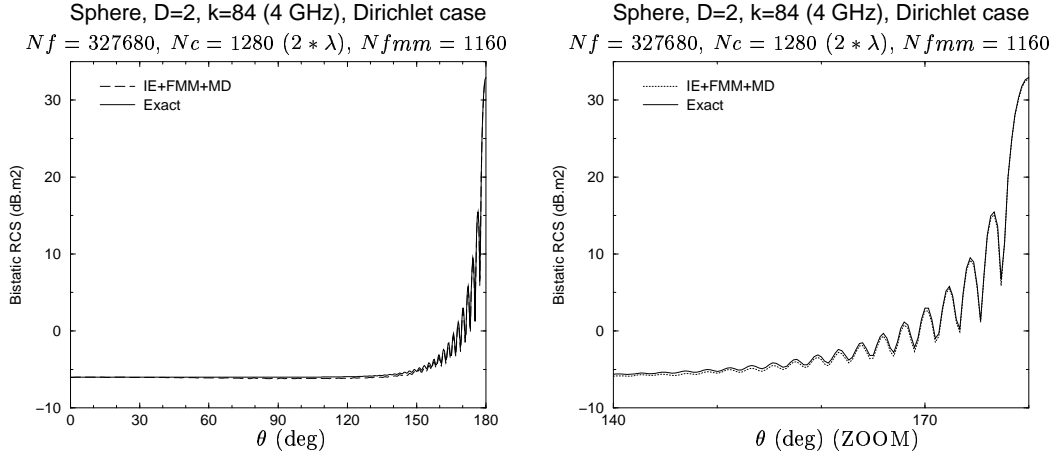


Figure 9:  $\mathcal{C}(\text{IE}+\text{MD}+\text{FMM})$ , Dirichlet case, 4 GHz

The quite good accuracy is given in the table below

Fig.	$k$	$N_f$	$N_c$	Memory	$Y_i X$	$Err(AD)$
8 a)	12	11520	180	51 MB	$6.6 \cdot 10^{-3}$	$1.2 \cdot 10^{-3}$
8 b)	24	46080	720	267 MB	$3 \cdot 10^{-3}$	$1 \cdot 10^{-3}$
9	84	327680	1280	2263 MB	$1.4 \cdot 10^{-3}$	$0.9 \cdot 10^{-3}$

Fig. 10 shows the results about CPU time and memory requirements with log-log curves.

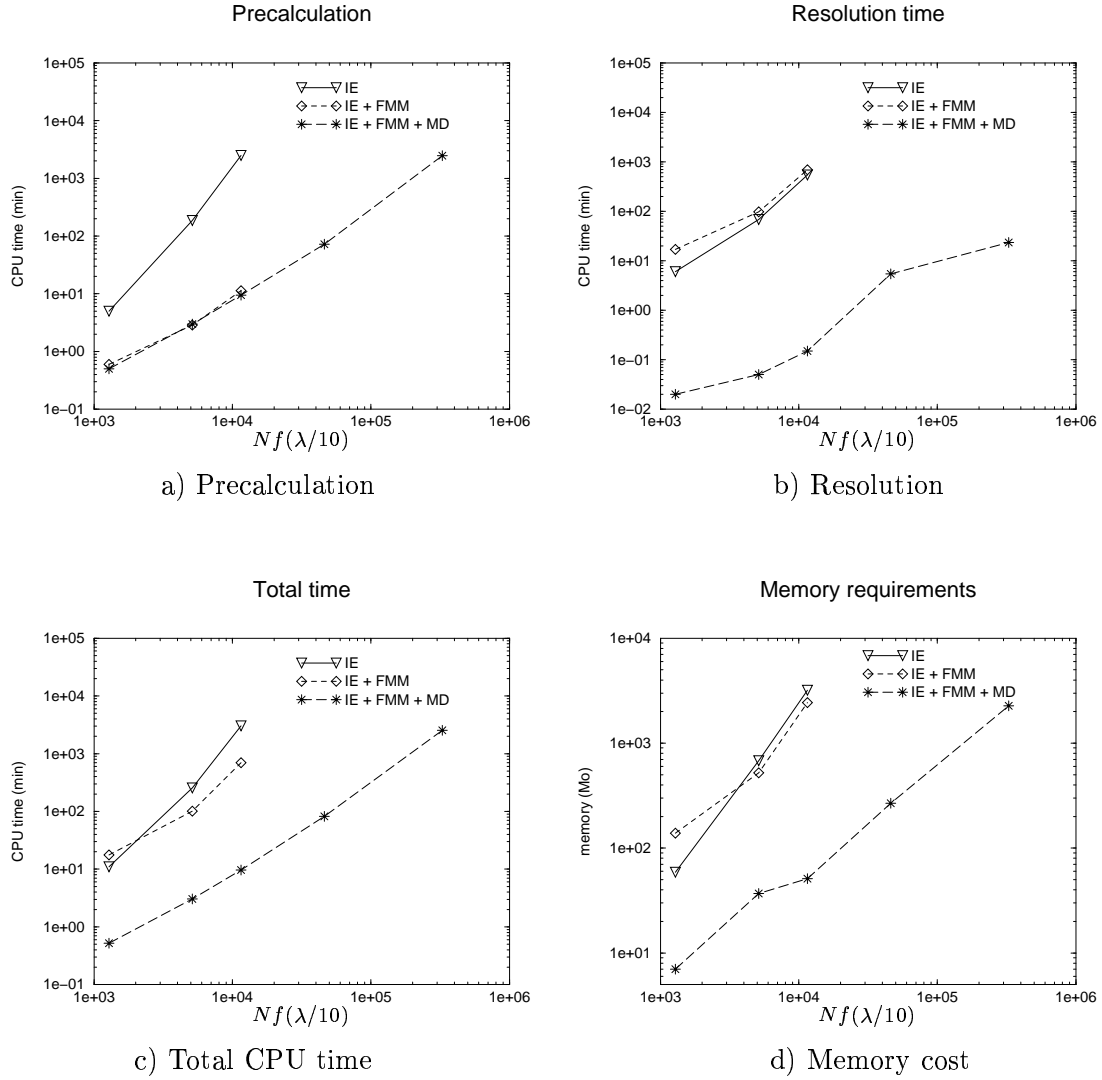


Figure 10: CPU time and memory requirements



Fig. 10 really shows that our new method is very efficient. We apply the code  $\mathcal{C}(\text{IE}+\text{MD}+\text{FMM})$  to the wave number  $\kappa = 84$  with the same requirements as the application of the code  $\mathcal{C}(\text{IE})$  to the wave number  $\kappa = 12$ . Considering a fine mesh with an average edge length about  $\lambda/10$ , we can choose a coarse mesh with an average edge length about  $\lambda/C_\kappa$  where  $C_\kappa$  decreases when  $\kappa$  increases. The case illustrated in Fig. 9 is really surprising with a coarse mesh where  $C_\kappa = 0.5$ , i.e. an average edge length about  $2\lambda$ . The frequencies considered are not large enough to validate the behaviour  $N_c \sim N_f^{1/3}$  estimated by the theory. However, we can plot a first curve concerning  $N_c$  as a function of  $N_f$  (see Fig. 11).

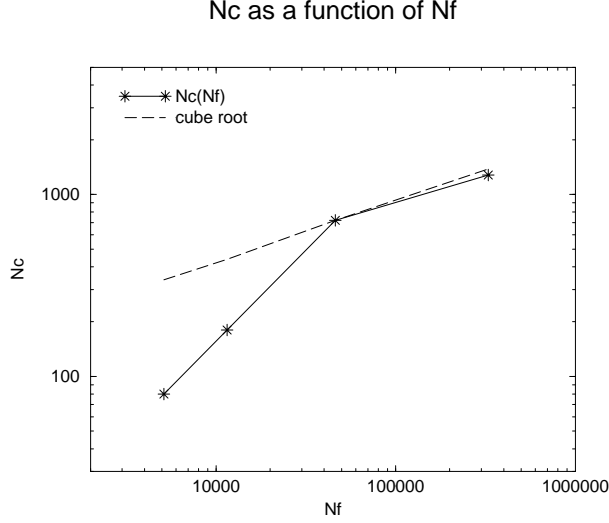


Figure 11:  $N_c(N_f)$

We can already see that the behaviour of  $N_c$  as a function of  $N_f$ , or as a function of the frequency, is promising. We give now information about the numbers of iterations in the iterative resolution. In the table, the numbers are given in the form  $a - b - c$  that are the numbers of iterations respectively of GC1, GC2 and JM.

$\kappa$	8	12	24
IE	11 - 8 - 19	10 - 8 - 20	
IE+FMM+MD	10 - 9 - 16	11 - 9 - 15	12 - 10 - 13

The numbers of iterations do not increase with  $\kappa$  and the new method does not damage the convergence of the iterative methods. Moreover, for the code  $\mathcal{C}(\text{IE}+\text{MD}+\text{FMM})$ , when the wave number increases, the number of iterations of JM decreases as well as the accuracy on  $\|Y_h - \imath X_h\|_2$  given previously.

Although results do not prove as good in both Neumann and Robin cases, probably because the approximation of the surface is of degree  $l = 1$  (see error estimations), they are still quite relevant. Fig. 12 and Fig. 13 give results for the Neumann boundary condition and the Robin boundary condition with the impedance  $Z = 1$ .

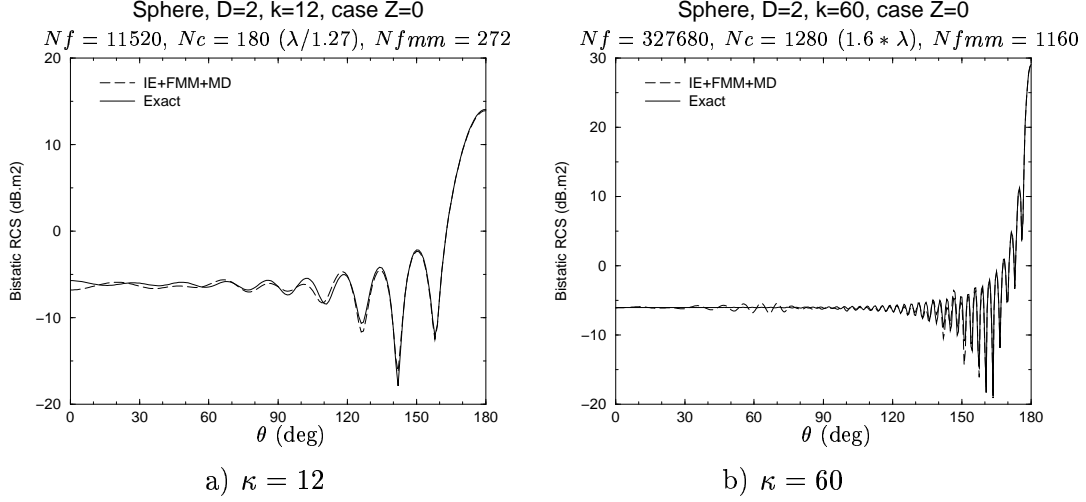


Figure 12:  $\mathcal{C}(\text{IE}+\text{MD}+\text{FMM})$ , Neumann case,  $\kappa = 12$  or 60

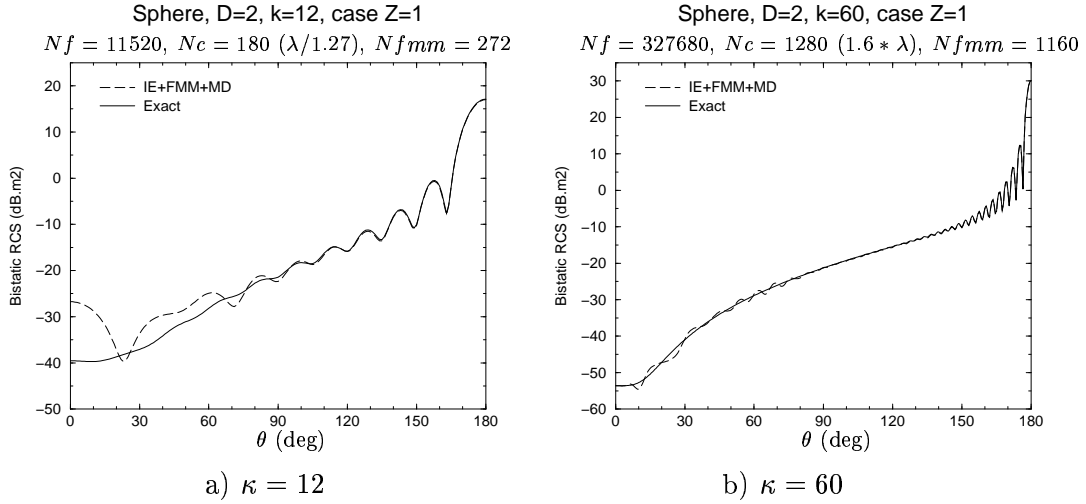


Figure 13:  $\mathcal{C}(\text{IE}+\text{MD}+\text{FMM})$ , Robin case,  $\kappa = 12$  or 60

As regards memory requirements and CPU time, both Neumann and Robin cases are similar to Dirichlet one. For the Neumann case, the accuracy is given in the table below

Fig.	$k$	$N_f$	$N_c$	$Y_i X$	$Err(AD)$
12 a)	12	11520	180	$2.2 \cdot 10^{-2}$	$3.7 \cdot 10^{-3}$
12 b)	60	327680	1280	$1.2 \cdot 10^{-2}$	$2.8 \cdot 10^{-3}$

For the Robin case, results are given in Fig. 13 and the accuracy is given as follows

Fig.	$k$	$N_f$	$N_c$	$Y_i X$	$Err(AD)$
13 a)	12	11520	180	$1.4 \cdot 10^{-2}$	$6.5 \cdot 10^{-2}$
13 b)	60	327680	1280	$1.8 \cdot 10^{-3}$	$3.3 \cdot 10^{-3}$

In this section, we have presented results such that the coarse mesh has an average edge length about  $\lambda/C_\kappa$  with  $C_\kappa$  becoming smaller and smaller for the same accuracy when  $\kappa$  increases. Thus the memory requirements and resolution time are less than the requirements of the other methods. Nevertheless, the matrix calculation deserves acceleration. We are hopeful that CPU time will be further reduced using a multilevel FMM instead of the one-level FMM.

## 7 Conclusion

The method we have developed couples two kinds of methods in order to speed up the solution of integral equations. Firstly, concepts of the geometrical and physical theories of diffraction enable us to reduce the size of the system considered, using the microlocal discretization introduced by T. Abboud, J.-C. Nédélec and B. Zhou. Secondly, concepts of the one-level FMM enable us to speed up the calculation of the matrix of the new system. Such a combination has resulted in a new method more efficient than the one-level FMM and more robust than the microlocal discretization which uses the theory of the stationary phase. Moreover, this coupling have been performed within a new formulation of the integral equations which is suitable for iterative resolution.

Numerical tests confirm the relevant reduction of both CPU time and memory cost. We have obtained good accuracies for resolutions based on rather coarse meshes, with an average edge length up to two wavelengths. However, both Neumann and Robin cases merit further improvements, considering a piecewise 2-degree polynomial surface in order to approximate the boundary of the object.

Moreover, we are contemplating the coupling with the multilevel FMM. It seems to further reduce the calculation of the matrix of the new system. It should result in an algorithm more efficient than the multilevel FMM thanks to the approximation of the phase function. For non-convex objects, we also plan to conduct a study based on the consideration of more directions in the phase approximation taking one's inspiration from works of A. de La Bourdonnaye. Besides, we will implement the new method within Maxwell's equations.

## Acknowledgments

I thank K. Mer-Nkonga, CEA-CESTA, and A. Bachelot, University of Bordeaux I for their contribution to this work.

## References

- [1] T. ABBOUD, J.-C. NÉDÉLEC, and B. ZHOU. Méthodes des équations intégrales pour les hautes fréquences. *C. R. Acad. Sci. Paris*, 318, serie I:165–170, 1994.
- [2] T. ABBOUD, J.-C. NÉDÉLEC, and B. ZHOU. Improvement of the Integral Equation Method for High Frequency Problems. *Third international conference on mathematical aspects of wave propagation phenomena, SIAM*, pages 178–187, 1995.
- [3] M. ABRAMOWITZ and I.A. STEGUN. *Handbook of Mathematical Functions with Formulas, Graphs, and Mathematical Tables*. John Wiley, New York, 1972.
- [4] V.M. BABIČ and V.S. BULDYREV. *Short-Wavelength Diffraction Theory*. Springer-Verlag, 1991.
- [5] N. BARTOLI and F. COLLINO. Integral Equations via Saddle Point Problem for Acoustic Problems. *M2AN*, 34(5):1023–1049, 2000.
- [6] D. BOUCHE and F. MOLINET. *Méthodes asymptotiques en électromagnétisme*. Springer-Verlag, 1994.
- [7] W.C. CHEW, J.M. JIN, C.-C. LU, E. MICHELSEN, and J.M. SONG. Fast Solution Methods in Electromagnetics. *IEEE Trans. on Antennas and Propag.*, 45(3):533–543, March 1997.
- [8] R. COIFMAN, V. ROKHLIN, and S. WANDZURA. The Fast Multipole Method for the Wave Equation: A Pedestrian Prescription. *IEEE Antennas and Propagation Magazine*, 35(3):7–12, June 1993.
- [9] E. DARRIGRAND. Fast Multipole Method and Microlocal Discretization for the Helmholtz Equation in Three Dimensions. In *Second International Conference on Boundary Integral Methods : Theory and Applications*. IMA - University of Bath, September 2000.
- [10] E. DARRIGRAND. Fast Multipole Method and Microlocal Discretization for the 3-D Helmholtz Equation. In *2001 IEEE AP-S International Symposium and USNC/URSI National Radio Science Meeting*. IEEE - MIT, July 2001.
- [11] E. DARVE. Fast Multipole Method: A Mathematical Study. *C. R. Acad. Sci. Paris*, 325, serie I(9):1037–1042, 1997.
- [12] E. DARVE. The Fast Multipole Method (I): Error Analysis and Asymptotic Complexity. *SIAM J. Numer. Anal.*, 38(1):98–128, 2000.
- [13] E. DARVE. The Fast Multipole Method: Numerical Implementation. *J. Comput. Phys.*, 160(1):195–240, 2000.

- [14] A. DE LA BOURDONNAYE. High Frequency Approximation of Integral Equations Modelizing Scattering Phenomena. *Mod. Math. et Anal. Num.*, 28(2):223–241, 1994.
- [15] A. DE LA BOURDONNAYE. Une méthode de discrétisation microlocale et son application à un problème de diffraction. *C. R. Acad. Sci. Paris*, 318, serie I:385–388, 1994.
- [16] B. DESPRÉS. Fonctionnelle quadratique et équations intégrales pour les problèmes d’onde harmonique en domaine extérieur. *M2AN*, 31(6):679–732, 1997.
- [17] L. GREENGARD and V. ROKHLIN. The Rapid Evaluation of Potential Fields in Three Dimensions. In *Vortex Methods in Lecture Notes in Mathematics, 1360, Springer Verlag*, pages 121–141, 1988.
- [18] L. GREENGARD and V. ROKHLIN. A New Version of the Fast Multipole Method for the Laplace Equation in Three Dimensions. *Acta Numerica*, 6:229–269, 1997.
- [19] L. HÖRMANDER. *The Analysis of Linear Partial Differential Operators I*. Springer-Verlag, 1983.
- [20] S. KOC, J.M. SONG, and W.C. CHEW. Error Analysis for the Numerical Evaluation of the Diagonal Forms of the Scalar Spherical Addition Theorem. *SIAM J. Numer. Anal.*, 36(3):906–921, April 1999.
- [21] R.B. MELROSE and M.E. TAYLOR. Near Peak Scattering and the Corrected Kirchhoff Approximation for a Convex Obstacle. *Adv. in Math.*, 55:242–315, 1985.
- [22] K. MER. The Fast Multipole Method Applied to a Mixed Integral System for Time-Harmonic Maxwell’s Equations. In *Second International Conference on Boundary Integral Methods : Theory and Applications*. IMA - University of Bath, September 2000.
- [23] J.-C. NÉDÉLEC. *Acoustic and Electromagnetic Equations, Integral Representation for Harmonic Problems*. Springer-Verlag, forthcoming.
- [24] J. RAHOLA. Diagonal Forms of the Translation Operators in the Fast Multipole Algorithm for Scattering Problems. *BIT*, 36(2):333–358, 1996.
- [25] V. ROKHLIN. Rapid Solution of Integral Equations of Scattering Theory in Two Dimensions. *J. Comput. Phys.*, 86(2):414–439, 1990.
- [26] V. ROKHLIN. Diagonal Forms of Translation Operators for the Helmholtz Equation in Three Dimensions. Research Report YALEU/DCS/RR-894, Yale University, March 1992.
- [27] J.M. SONG and W.C. CHEW. Multilevel Fast Multipole Algorithm for Solving Combined Field Integral Equations of Electromagnetic Scattering. *Microwave Opt. Tech. Letter*, 10(1):14–19, September 1995.
- [28] J.M. SONG, C.-C. LU, and W.C. CHEW. Multilevel Fast Multipole Algorithm for Electromagnetic Scattering by Large Complex Objects. *IEEE Trans. on Antennas and Propag.*, 45(10):1488–1493, October 1997.

- [29] J.M. SONG, C.-C. LU, W.C. CHEW, and S.W. LEE. Fast Illinois Solver Code (FISC) Solves Problems of Unprecedented Size at the Center for Computational Electromagnetics, University of Illinois. Research Report CCEM-23-97, University of Illinois, Urbana Champaign, IL, August 1997.
- [30] B. STUPFEL. A Hybrid Finite Element and Integral Equation Domain Decomposition Method for the Solution of the 3-D Scattering Problem. *J. Comput. Phys.*, to appear.
- [31] B. STUPFEL and B. DESPRÉS. A domain decomposition method for the solution of large electromagnetic scattering problems. *J. Electromag. Waves and Appl.*, 1999.
- [32] M.E. TAYLOR. *Pseudodifferential Operators*. Princeton University Press, 1981.
- [33] R.L. WAGNER and W.C. CHEW. A Ray-Propagation Fast Multipole Algorithm. *Microwave Opt. Tech. Letter*, 7(10):435–438, July 1994.
- [34] B. ZHOU. *Méthode des équations intégrales pour la résolution des problèmes de diffraction à hautes fréquences*. Thèse de doctorat, Université Paris XI, Novembre 1995.